www.sciencemag.org/cgi/content/full/science.aad5143/DC1

Supplementary Materials for

In vivo genome editing improves muscle function in a mouse model of Duchenne muscular dystrophy

Christopher E. Nelson, Chady H. Hakim, David G. Ousterout, Pratiksha I. Thakore, Eirik A. Moreb, Ruth M. Castellanos Rivera, Sarina Madhavan, Xiufang Pan, F. Ann Ran, Winston X. Yan, Aravind Asokan, Feng Zhang, Dongsheng Duan, Charles A. Gersbach*

*Corresponding author. E-mail: charles.gersbach@duke.edu

Published 31 December 2015 on *Science* First Release
DOI: 10.1126/science.aad5143

This PDF file includes:

Materials and Methods

Molecular Cloning and AAV Production

A *Staphylococcus aureus* Cas9 (SaCas9) expression plasmid containing an H1-driven gRNA cassette (pTRSaCas9-H1) was received as a gift from the Zhang lab (*20*). The CMV-SaCas9-polyA was transferred to a new plasmid without ITRs for stability in cell culture experiments (pSaCas9). The CMV-SaCas9-polyA was cloned into the empty ITR-plasmid to make pTRSaCas9 that contains the SaCas9 expression cassette and no gRNA cassette. A new codon optimized version of the CMV-SaCas9-H1-gRNA is available through Addgene (Zhang Lab#61591/61592). pgRNA *(20, 44)* was used with BbsI cloning to screen guides *in vitro*. For the AAV transfer plasmid, two gRNAs were cloned into a pTR-eGFP backbone replacing the CMV with the gRNA cassettes. Briefly, gRNA1 was amplified through PCR with F-AAV-gRNA1/R-AAV-gRNA1 and gRNA2 was amplified through PCR with F-AAV-gRNA2/R-AAV-gRNA2. Both gRNAs were cloned in sequentially to produce pTRgRNAs. The promoterless eGFP was left as a stuffer to keep the packaging size above the minimum 3.5 kb for efficient packaging.

AAV Production

ITRs were verified by SmaI digest before production (**Fig. S15**). pTRSaCas9 and pTRgRNAs were used to generate stock AAV8 in two separate batches by the University of North Carolina – Chapel Hill Viral Vector Core and titered by dot blot. Titers were provided at $4.7x10^{13}$ vp/mL (pTRSaCas9) and $2.8x10^{13}$ vp/mL (pTRgRNAs) dialyzed w/350 mM NaCl & 5% D-Sorbitol in PBS.

Cell Culture and gRNA Screening

A panel of guide RNAs (**Fig. S1**) were designed against intron 22 and intron 23 of the mouse DMD gene and compared for activity by the Surveyor assay. C2C12 mouse myoblasts were obtained from American Type Culture Collection (ATCC) and maintained in DMEM, high glucose, pyruvate (Gibco) supplemented with 20% fetal bovine calf serum and 1% penicillin/ streptomycin and maintained at 37°C at 5% CO_2. C2C12 cells were transfected with 5 µg of each plasmid (Cas9 and gRNA) by electroporation with a Gene Pulser XCell (BioRad) in PBS (Sigma) using previously optimized conditions (*22*). Briefly, BioRad 2 mm gap electroporation cuvettes with 1 million cells in 200 µL PBS were electroporated at 1000 µF and 160 V. Cells were immediately immersed in complete media and transferred into a single well of a 6 well plate. Cells were incubated for 72h and genomic DNA was isolated with a DNeasy kit (Qiagen). PCR across regions of interest (Surveyor Primers, **Table S1**) was performed with the Invitrogen AccuPrime High Fidelity PCR kit for 35 cycles. 8 µL of PCR product was incubated with the Surveyor Nuclease according to kit instructions (*45*). DNA was then denatured in SDS at 65°C and electrophoresed on TBE gels (Life Technologies) for 30 min at 200V. Gels were stained with ethidium bromide and imaged on a ChemiDoc™ chemiluminescence system (BioRad). Selected gRNAs were examined for off-target interactions in the mouse genome with an online search algorithm (*46*) to ensure that no potential off-target sites existed in the mouse genome with less than three mismatches in the target sequence.

Intramuscular Injection of AAV-CRISPR

The animal studies herein were conducted with adherence to the guidelines for the care and use of laboratory animals of the National Institutes of Health (NIH). All the experiments with animals were approved by the Institutional Animal Care and Use Committee (IACUC) at Duke

University or University of Missouri. 6-8 week old male *mdx* mice (Jackson Labs: 001801) were anesthetized and maintained at 37 °C. The tibialis anterior (TA) muscle was prepared and injected with 30-40 µL of AAV solution (5.6×10^{11} - 7.46×10^{11} vg/vector/mouse) or saline into the right and left TA, respectively. After 8 weeks or 6 months, mice were euthanized by CO_2 inhalation and tissue was collected into RNALater® (Life Technologies) for DNA, RNA, or protein analysis.

Intraperitoneal Injection of AAV-CRISPR

Two day-old male *mdx* neonates were injected into the intraperitoneal space with 15 µL of AAV8 solution (2.8×10^{11} vg/vector/mouse). After 7 weeks, mice were euthanized by CO_2 inhalation and tissue was collected into RNALater® (Life Technologies) for DNA and protein analysis or 30% sucrose for frozen tissue sections.

Intravenous injection of AAV-CRISPR into adult *mdx* mice

6 week old male *mdx* mice were injected via the tail vein with 200 µL of AAV8 solution (2.7e12 vg/vector/mouse). After 8 weeks, mice were euthanized by CO_2 inhalation and tissue was collected into RNALater® (Life Technologies) for DNA and protein analysis or 30% sucrose for frozen tissue sections.

Genomic DNA Analysis

Mouse muscles were digested in ALT buffer and proteinase K for 4h at 56 °C with intermittent mixing. DNEasy kit (Qiagen) was used to collect genomic DNA. Endpoint PCR was performed with primers flanking CRISPR cut sites that amplify a 1638bp region (In22-gRNA1/6-F and In23-gRNA2-R). PCR products were electrophoresed in a 1% agarose gel and viewed on a BioRad GelDoc imager to observe the 1638 bp intact band and the expected 467 bp deletion product (full gel **Fig. S16**). Gel bands were extracted with a gel extraction kit (Qiagen) and further purified by PCR purification (Qiagen) for Sanger sequencing (Eton Bioscience). Quantitative droplet digital PCR (ddPCR) was performed on samples using a QX200™ Droplet Digital™ PCR System with QX200™ ddPCR™ EvaGreen Supermix (BioRad). Two primer sets were designed including primers specific for the intact dystrophin gene (dPCR-intact-F/dPCR-R) and primers specific the deletion product (dPCR-del-F/dPCR-R). The full data panel is available in **Fig. S17**.

Deep Sequencing

PCR of genomic DNA from 6 untreated control TA muscles and 6 treated TA muscles was completed using primers designed against the two target regions and 20 candidate off-target sites (**Table S1**). A second round of PCR was used to add Illumina flowcell binding sequences and experiment-specific barcodes on the 5' end of the primer sequence (**Table S1**). The resulting PCR products were pooled and sequenced with 150 bp paired-end reads on an Illumina MiSeq instrument. Samples were demultiplexed according to assigned barcode sequences, and Illumina adapter and primer sequences were trimmed from reads. Indel analysis was performed as previously described (*21, 24*). Briefly, because expected PCR products were <250 bp in length, the 3' ends of paired-end reads overlapped. This overlap was used to generate a consensus PCR amplicon for each paired-end read via single ungapped alignment (parameterized to score each match as 5 and each mismatch as -4). Trimmed fragments were aligned to the mm10 reference genome using BLAT. Each of the aligning fragments was then aligned to the reference genome sequence of the expected PCR product using a global affine alignment with the following parameterization: match=5, mismatch=−4, gap open=−5, gap extend=−2. Any fragment that did

not have greater than 60% identity with an expected PCR product or that had a top-scoring BLAT alignment that was different than the expected PCR product was discarded from downstream analysis. Alignments were then trimmed to a 20 bp window centered three base pairs 5' of the PAM, the predicted site of SaCas9 nuclease activity. Indel (insertion and/or deletion) statistics were gathered from these windows separately for each treatment/control by counting gaps in the query and subject sequences of the resulting truncated alignments and tabulating numbers of fragments having any indels in these windows.

RNA analysis

RNA was extracted from tissues stabilized in RNALater® (Invitrogen) using a Tissue Lyser (Qiagen) and the RNeasy Plus Universal Kit (Qiagen). cDNA was synthesized using SuperScript® VILO cDNA Synthesis Kit and Master Mix (Life Technologies). Endpoint PCR was performed with Accuprime polymerase and electrophoresed in a 1% agarose gel (full gel **Fig. S18**). Gel bands were extracted with a gel extraction kit (Qiagen) and further purified by PCR purification kit (Qiagen) for Sanger sequencing. Quantitative digital drop PCR (ddPCR) was performed on samples using a QX200™ Droplet Digital™ PCR System with QX200TM ddPCRTM EvaGreen Supermix (BioRad). Two primer sets were designed including a primer set specific for the total dystrophin RNA (dPCR-ex22-F and dPCR-ex24/25-R) and the Δ23 transcript (dPCR-ex22/24-F and dPCR-ex24/25R). Full data panel is available in **Fig. S19**.

Protein analysis and western blot

Muscle biopsies were disrupted with a probe sonicator (Fisher Scientific FB50) in RIPA buffer (Sigma) with a proteinase inhibitor cocktail (Roche) and incubated for 30 min on ice with intermittent vortexing. Samples were centrifuged at 16000xg for 30 min at 4°C and the supernatant was isolated and quantified with a bicinchronic acid assay (Pierce). Protein isolate was mixed with NuPAGE loading buffer (Invitrogen) and 5% β-mercaptoethanol and boiled at 100°C for 10min. Samples were flash frozen in liquid nitrogen for future analysis. 25 µg total protein per lane were loaded into 4-12% NuPAGE Bis-Tris gels (Invitrogen) with MOPS buffer (Invitrogen) and electrophoresed for 30 min at 200 V. Protein was transferred to nitrocellulose membranes for 1 hour in 1X tris-glycine transfer buffer containing 10% methanol and 0.01% SDS at 4°C at 400 mA. The blot was blocked overnight at 4°C in 5% milk-TBST. Blots were probed with Dys-2 (1:100, clone Dy8/6C5, IgG1; Novocastra, Newcastle, UK), anti-HA (abcam), MANDYS8 (1:200, Sigma D8168), rabbit anti-GAPDH (1:5000, Cell Signaling 2118S), or anti-skeletal myosin heavy chain antibody (1:5000, Sigma MF20) for 1 hour in 5% milk-TBST at room temperature. Blots were then incubated with mouse or rabbit horseradish peroxidase-conjugated secondary antibodies (Santa Cruz) for 30 min in 5% milk-TBST. Blots were visualized using Western-C ECL substrate (Biorad) on a ChemiDoc chemiluminescent system (Biorad). The full blots are available in **Fig. S20**.

Histological stains

TA muscles were carefully dissected and embedded in OCT using liquid nitrogen-cooled isopentane. 10 µm sections were cut onto pre-treated histological slides. Hematoxylin and eosin was used to reveal general muscle histopathology. Macrophage and neutrophil infiltration were detected by immunohistochemical staining with a mouse macrophage-specific antibody (#RM2920, 1:200; clone CI:A3-1, IgG2b; Caltag Laboratories, Burlingame, CA) and a rat anti-mouse Ly6-G antibody (1:800; BD Pharmingen, San Diego, CA), respectively. Dystrophin was

detected with a rabbit polyclonal antibody (1:600) against the N-terminal domain of dystrophin. DGC components were evaluated with mouse monoclonal antibody against α-sarcoglycan (Ad1/20A6, 1:50, Vector Laboratories, Burlingame, CA), β-sarcoglycan (βSarc/5B1, 1:50; Novocastra, Buffalo Grove, IL), γ-sarcoglycan (35DAG/21B5, 1:50; Vector Laboratories, Burlingame, CA), β-dystroglycan (43DAG1/8D5, 1:50; Novocastra, Buffalo Grove, IL), syntrophin (ab11187, 1:200; Abcam, Cambridge, MA) and dystrobrevin (23/Dystrobrevin, 1:200; BD Biosciences, San Diego, CA). Laminin was detected with a rabbit polyclonal antibody (L9393, 1:200, Sigma, Saint Louis, MO). Utrophin was examined with a mouse monoclonal antibody against the N-terminus of utrophin (1:20, Vector Laboratories, Burlingame, CA). nNOS expression was revealed by nNOS activity staining as previously described (*47*) and by immunostaining with a rabbit polyclonal antibody against the C-terminal domain of nNOS (1:2000, Santa Cruz, Dallas, TX). Embryonic myofibers were detected with a monoclonal antibody against embryonic myosin heavy chain (eMHC) (1:250; Developmental Studies Hybridoma Bank, Iowa City, IA). The myosin heavy chain isoforms were identified using mouse monoclonal antibodies generated from hybridoma cells against Type I, IIa and IIb MyHC (Developmental Studies Hybridoma Bank, Iowa City, IA). The HA tag fused to C-terminus domain of the SaCas9 gene was detected with a rat monoclonal antibody (3F10, 1:50, Roche, Pleasanton, CA). Dystrophin-positive fibers were manually counted from the representative images in **Fig. S21**. Control injections of Cas9-AAV only or gRNA-AAV were stained for dystrophin and are reported in **Fig. S22.**

In situ evaluation of TA muscle contractile properties

TA muscle contractile properties were measured as previously described (*48*) using the Aurora Scientific *in situ* muscle test system. Briefly, the mouse was anesthetized and the body core temperature was maintained at 37°C using a heated platform. The hind limb was shaved and the TA muscle was surgically exposed and the distal tendon was tied at the muscle tendon junction using a 4-0 suture line (SofSilk USSC Sutures, Norwalk, CT). Another suture line was attached to the patella ligament. The sciatic nerve was carefully dissected, tied to a suture, and cut at the proximal end. The mouse was placed prone on a custom made platform and the knee was secured to a fixed post using the patella suture line. The sciatic nerve was placed on custom made electrode and secured using the suture line. The distal end of the TA muscle was secured to the lever arm of the force transducer. The exposed hind limb muscles were covered with a warm Ringer's buffer soaked Kimwipes. Throughout the experiment, the muscles were constantly superfused with warm oxygenated Ringer's buffer. After 5 minutes equilibration, the muscle was warmed up and optimal length (Lo), current and stimulation time were determined. Twitch tension (Pt) and maximal isometric tetanic force (Po) were measured. The muscle was allowed to relax for 3 min before 10 cycles of eccentric contractions were applied with a 1 min rest between each cycle. Relative force loss was later determined for each cycle. Data were recorded and analyzed using the Lab-View based DMC and DMA software (Version 3.12, Aurora Scientific, Aurora, ON, Canada). At the end of each experiment, the distal TA tendon was removed and TA muscle weight was measured. The muscle cross sectional area was determined based on a muscle density of 1.06 g/cm^3 and fiber length to Lo ratio of 0.6.

Statistical Analysis

Sample sizes for animal studies were designed based on previous studies of dystrophin-mediated muscle function recovery (*48*). All intact samples were included in data analysis and no sample was excluded. Student t-tests were used to determine significance of single comparisons in Figures

1-3. Repeated measures ANOVA was used to validate overall treatment effect in the eccentric contractility test (Figure 3d). All of the variation reported in Figures 1-3 show standard error between biological replicates. Randomization and blinding were not used as each biological replicate has a built-in negative treated contralateral control. Restoration of dystrophin protein has been duplicated in multiple laboratory experiments. For muscle contractility experiments, mice were injected on different days and analyzed on different days (n=7).

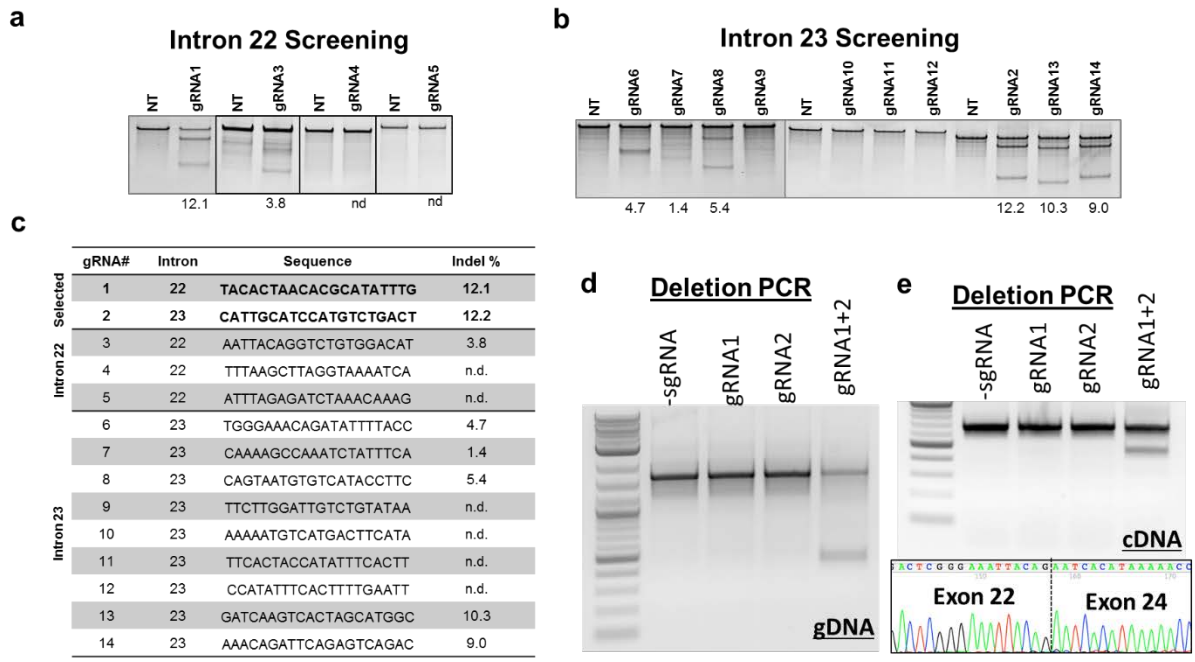

	gRNA#	Intron	Sequence	Indel %
Selected	1	22	**TACACTAACACGCATATTTG**	**12.1**
	2	23	**CATTGCATCCATGTCTGACT**	**12.2**
Intron 22	3	22	AATTACAGGTCTGTGGACAT	3.8
	4	22	TTTAAGCTTAGGTAAAATCA	n.d.
	5	22	ATTTAGAGATCTAAACAAAG	n.d.
Intron 23	6	23	TGGGAAACAGATATTTTACC	4.7
	7	23	CAAAAGCCAAATCTATTTCA	1.4
	8	23	CAGTAATGTGTCATACCTTC	5.4
	9	23	TTCTTGGATTGTCTGTATAA	n.d.
	10	23	AAAAATGTCATGACTTCATA	n.d.
	11	23	TTCACTACCATATTTCACTT	n.d.
	12	23	CCATATTTCACTTTTGAATT	n.d.
	13	23	GATCAAGTCACTAGCATGGC	10.3
	14	23	AAACAGATTCAGAGTCAGAC	9.0

Fig. S1.

In vitro characterization of *Staphylococcus aureus* Cas9 (SaCas9) gRNAs. Plasmid electroporation of C2C12 mouse skeletal myoblasts was used to screen gRNAs. (**a**) 4 gRNAs were screened in intron 22 with gRNA1 displaying the highest activity at 12.1% indel formation. (**b**) For intron 23, 10 gRNAs were screened with gRNA2 displaying the highest activity at 12.2% indel formation. (**c**) gRNA sequences are shown in the table. (**d**) Combined activity of gRNA1 and gRNA2 creates genomic deletions. (**e**) Reverse transcription and PCR of the mRNA transcript also indicates the removal of exon 23 in C2C12 cells as evidenced by gel electrophoresis and Sanger sequencing of the extracted smaller band.

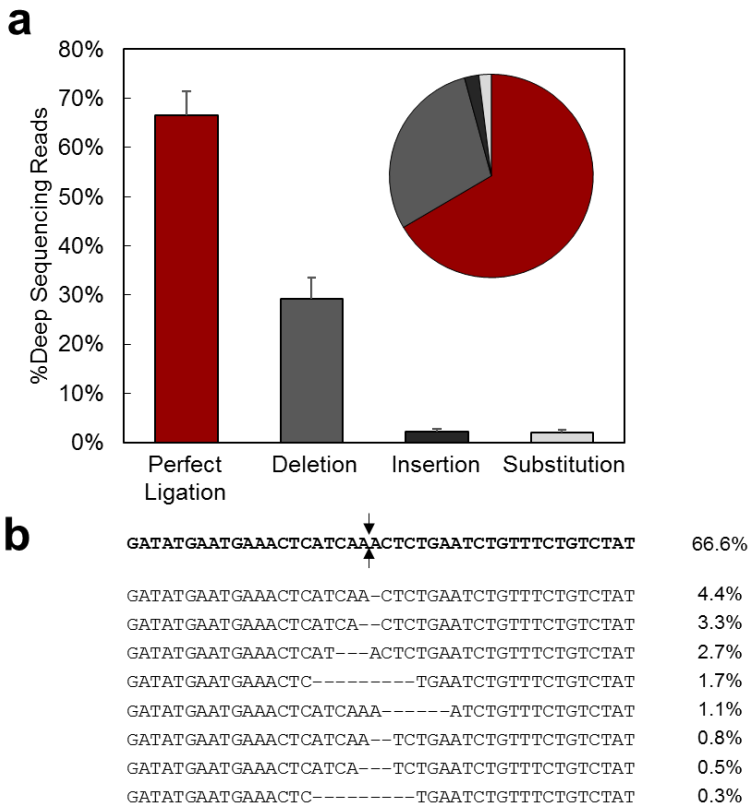

Fig. S2

Cas9-mediated deletion has a strong preference for perfect ligation of cut sites. a) The distribution of deletion products shows ~67% perfect deletions with ~30% deletions within the cut site and small fractions of insertions or substitutions. **b**) The perfect ligation product with cut site marked with arrows and the eight most prevalent resulting sequences.

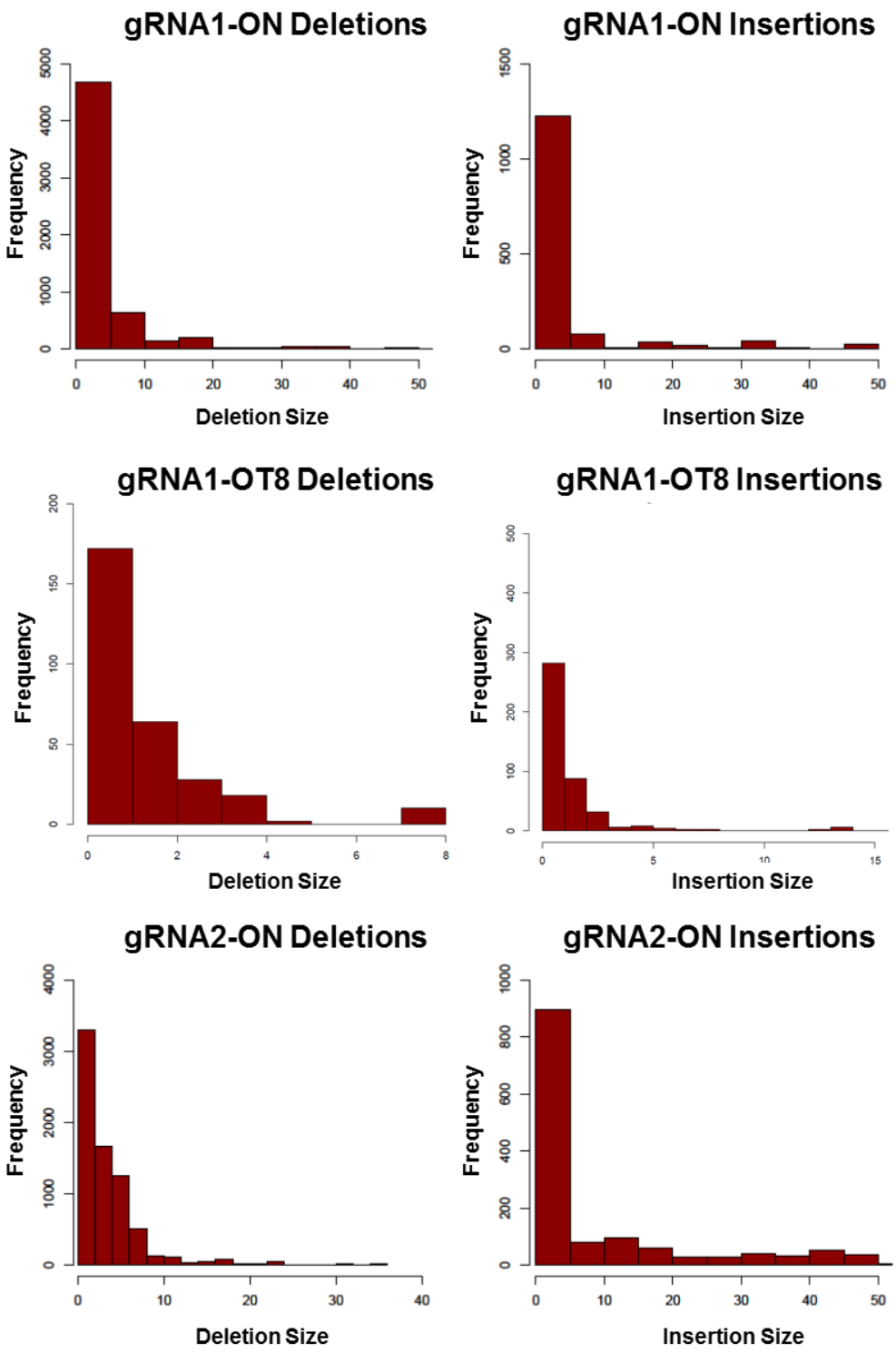

Fig. S3

Distribution of indel sizes in selected target regions from mouse skeletal muscle by deep sequencing.

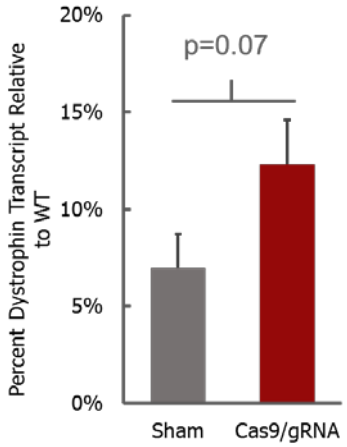

Fig. S4.

Total dystrophin RNA levels relative to WT. ddPCR suggests that Cas9/gRNA treated mdx mice have higher overall levels of dystrophin RNA, indicating Δ23 transcripts avoid nonsense-mediated decay caused by the premature stop codon in exon 23.

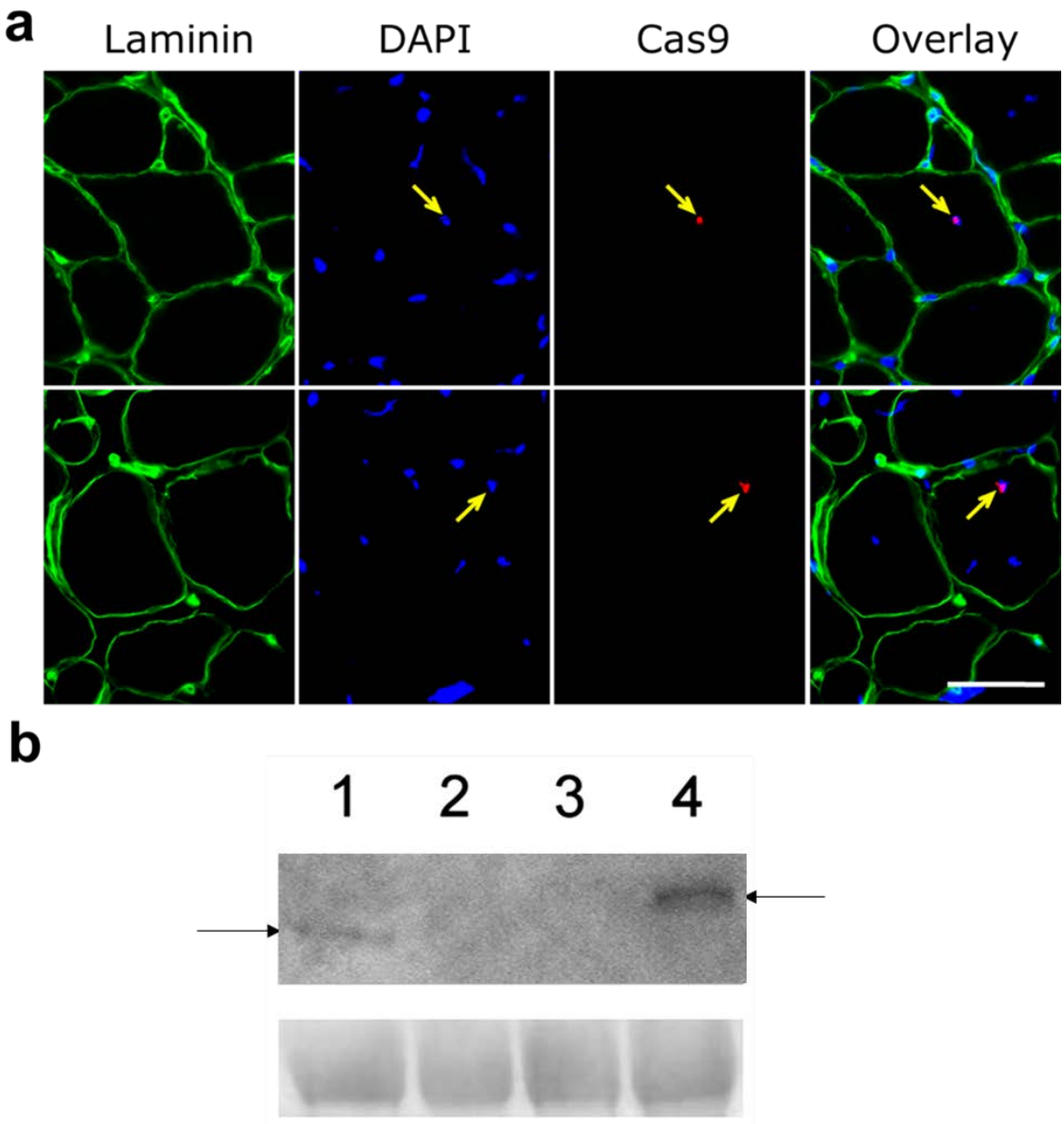

Fig. S5.

Detection of SaCas9 in treated muscle. **(a)** Two representative photomicrographs showing SaCas9 expression in the nucleus of AAV infected muscle. Laminin immunofluorescence staining marks the sarcolemma. Myonuclei are stained with DAPI. SaCas9 is revealed with immunofluorescence staining against the HA epitope tag on the C terminus of SaCas9. Scale bar, 50 μm. **(b)** Detection of the HA tag on SaCas9 in whole muscle lysate by western blot. 1- mdx mice treated with the AAV expressing HA-tagged Cas9, 2 – untreated mdx mice, 3 - untreated BL10 mice, 4 - mdx mice treated with an AAV vector encoding HA-tagged micro-dystrophin.

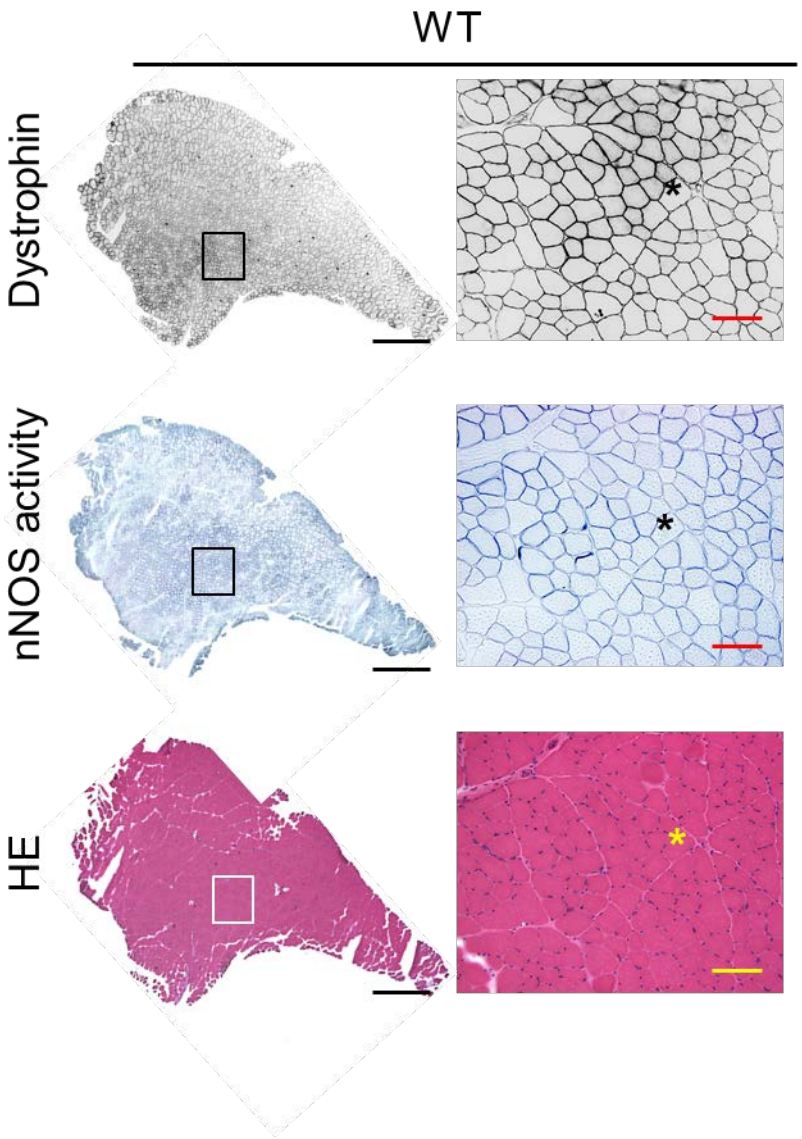

Fig. S6.

Wild-type (WT) control for Figure 3a-c. Asterisk, same myofiber in the serial sections. Scale bar = 600 μm in full-view images, and 100 μm in high-power images.

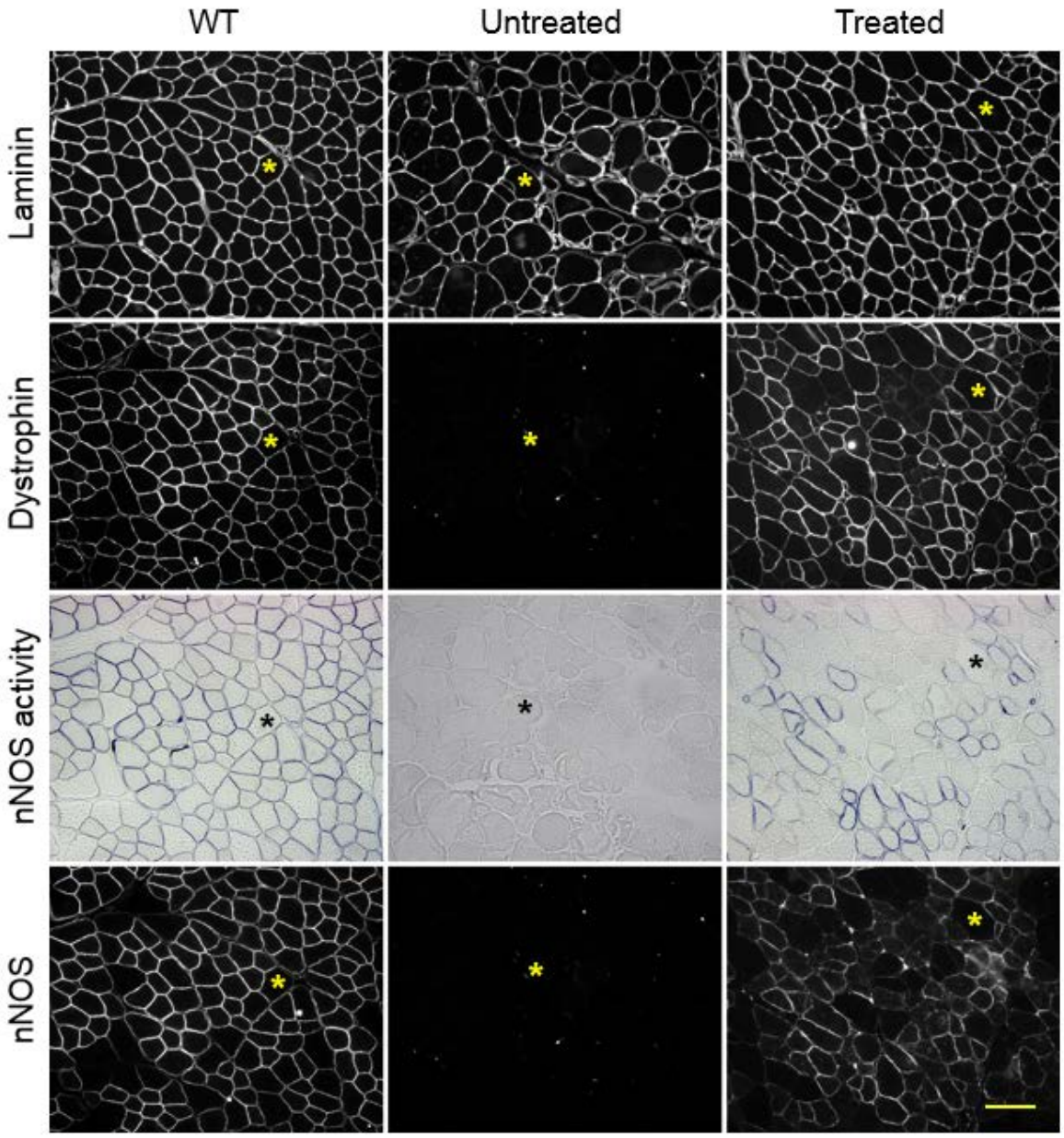

Fig. S7.

Representative photomicrographs of immunofluorescence staining for laminin, dystrophin, nNOS enzymatic activity, and nNOS - Serial muscle sections were stained for laminin (to mark muscle cell membrane), dystrophin, nNOS with the indicated rabbit polyclonal antibody. **Asterisk,** the same myofiber in serial sections. **Scale bar:** 100 μm.

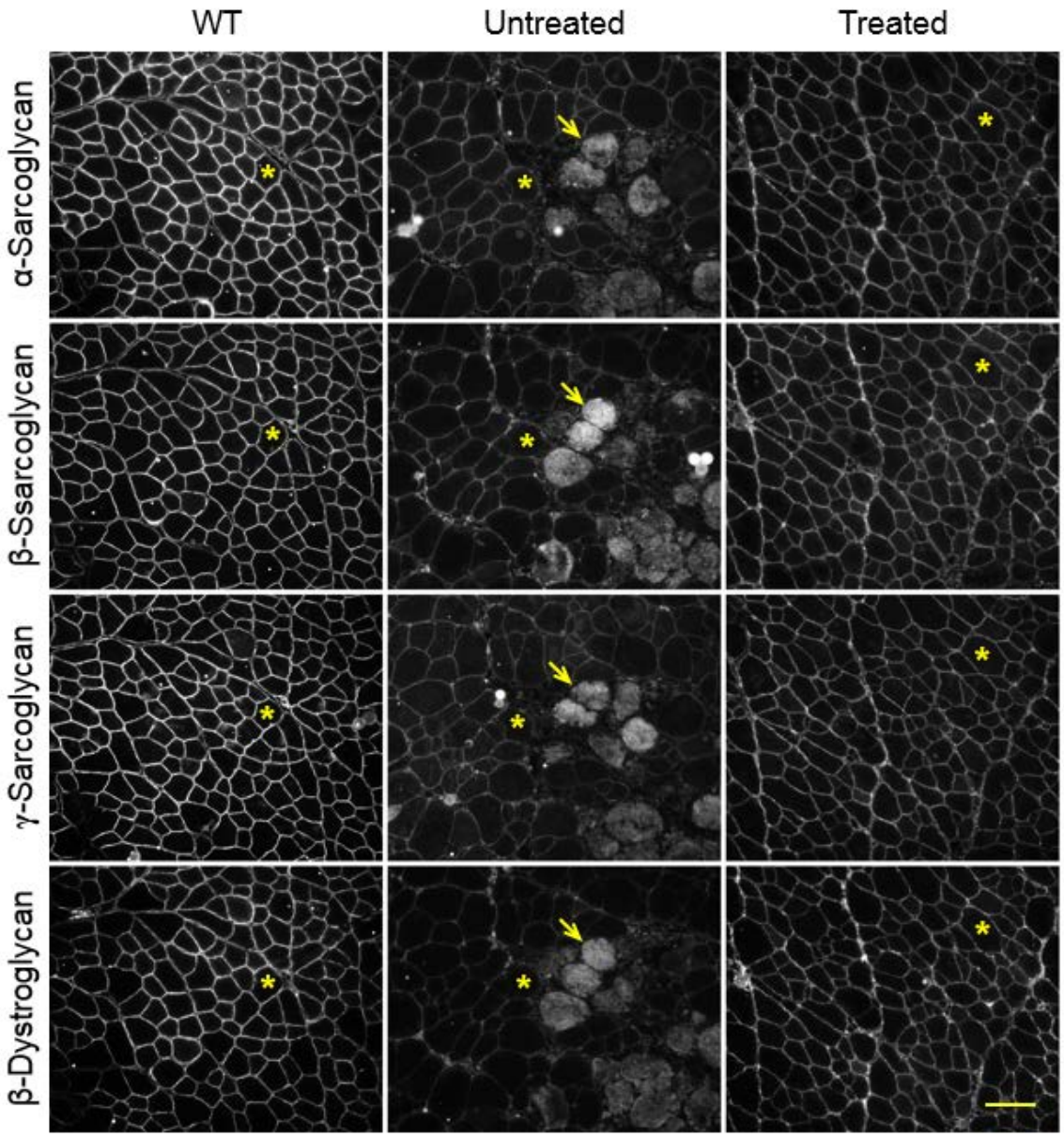

Fig. S8.

Representative photomicrographs of immunofluorescence staining for components of dystrophin-associated glycoprotein complex (α-sarcoglycan β-sarcoglycan γ-sarcoglycan, β-dystroglycan) using the indicated mouse monoclonal antibody. Arrow, Strong cytosolic staining reflecting accumulation of mouse immunoglobulin (IgG) in damaged myofibers. IgG reacts with the fluorescein-conjugated mouse anti-mouse antibody (secondary antibody). **Asterisk,** the same myofiber in serial sections. **Scale bar,** 100 μm.

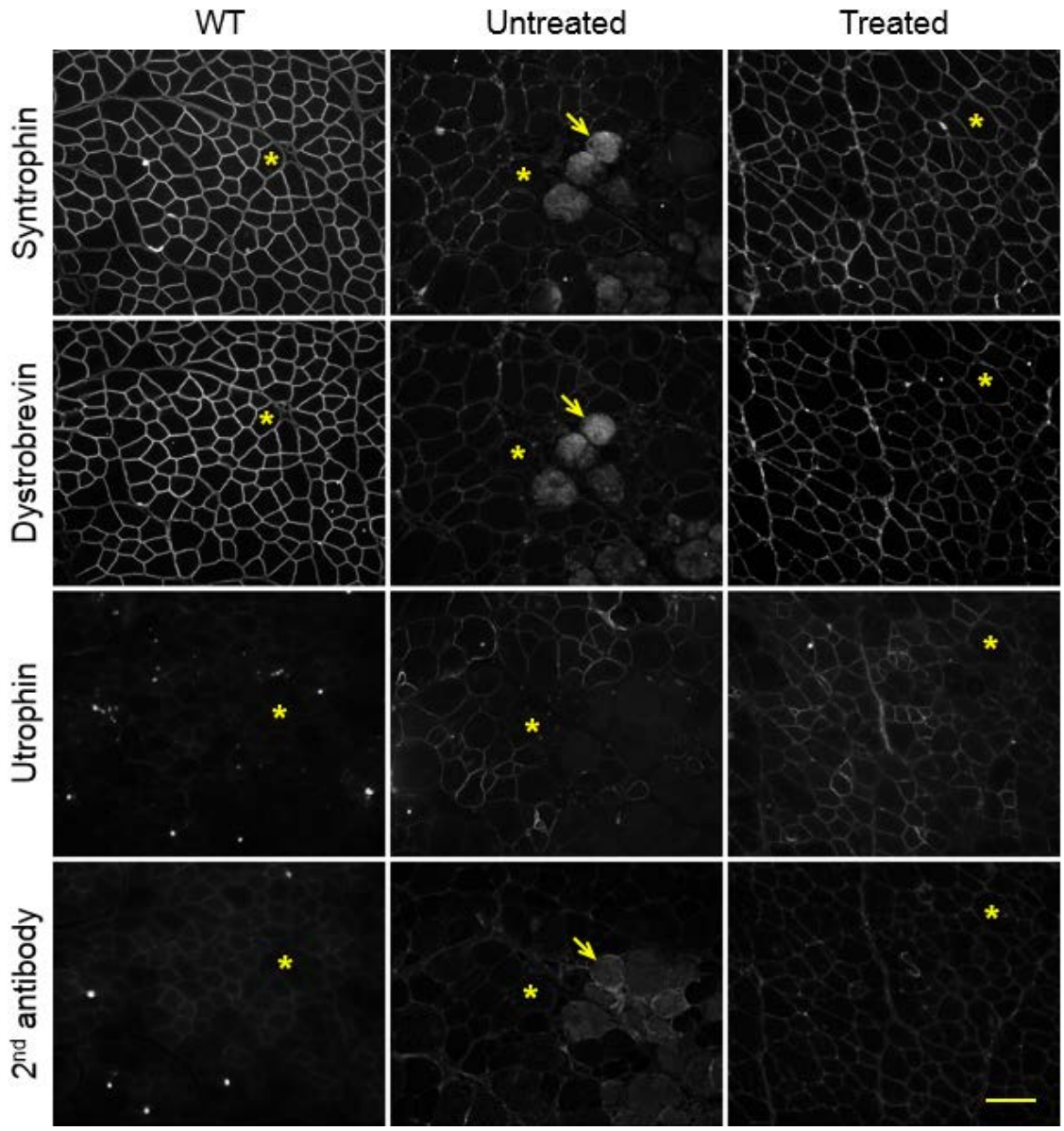

Fig. S9.

Representative photomicrographs of immunofluorescence staining for syntrophin, dystrobrevin and utrophin using the indicated mouse monoclonal antibody. The bottom row shows background staining with the secondary antibody alone (applicable to Supplemental Figure 6 and 7). **Arrow,** Strong cytosolic staining reflecting accumulation of mouse immunoglobulin (IgG) in damaged myofibers. IgG reacts with the fluorescein-conjugated mouse anti-mouse antibody (secondary antibody). **Asterisk,** the same myofiber in serial sections. **Scale bar,** 100 μm.

Cas9/gRNA-treated mice

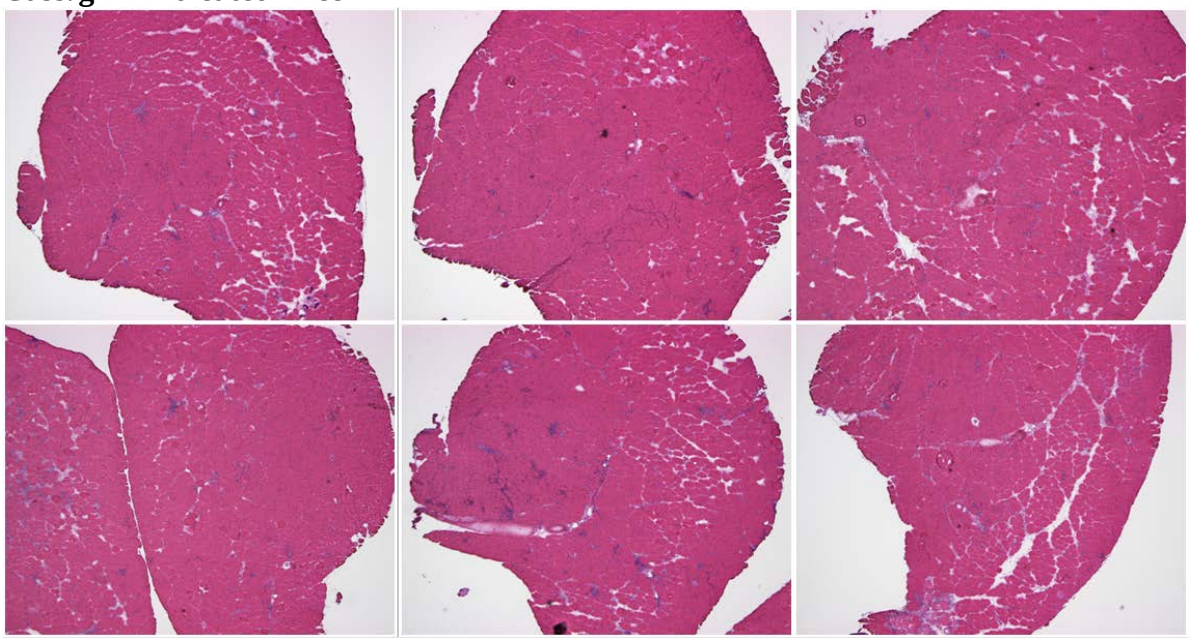

Sham injected mice

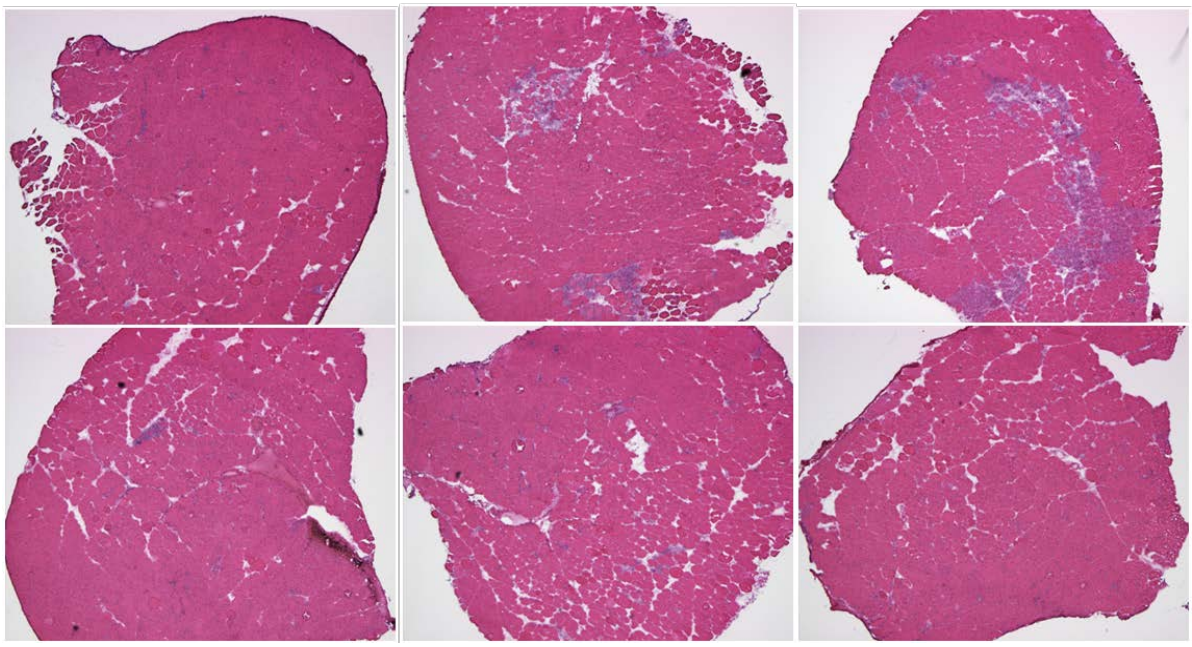

Fig. S10.

Representative photomicrographs of H&E stained muscle sections from CRISPR/gRNA treated muscles (top two rows) and sham injected muscles (bottom two rows).

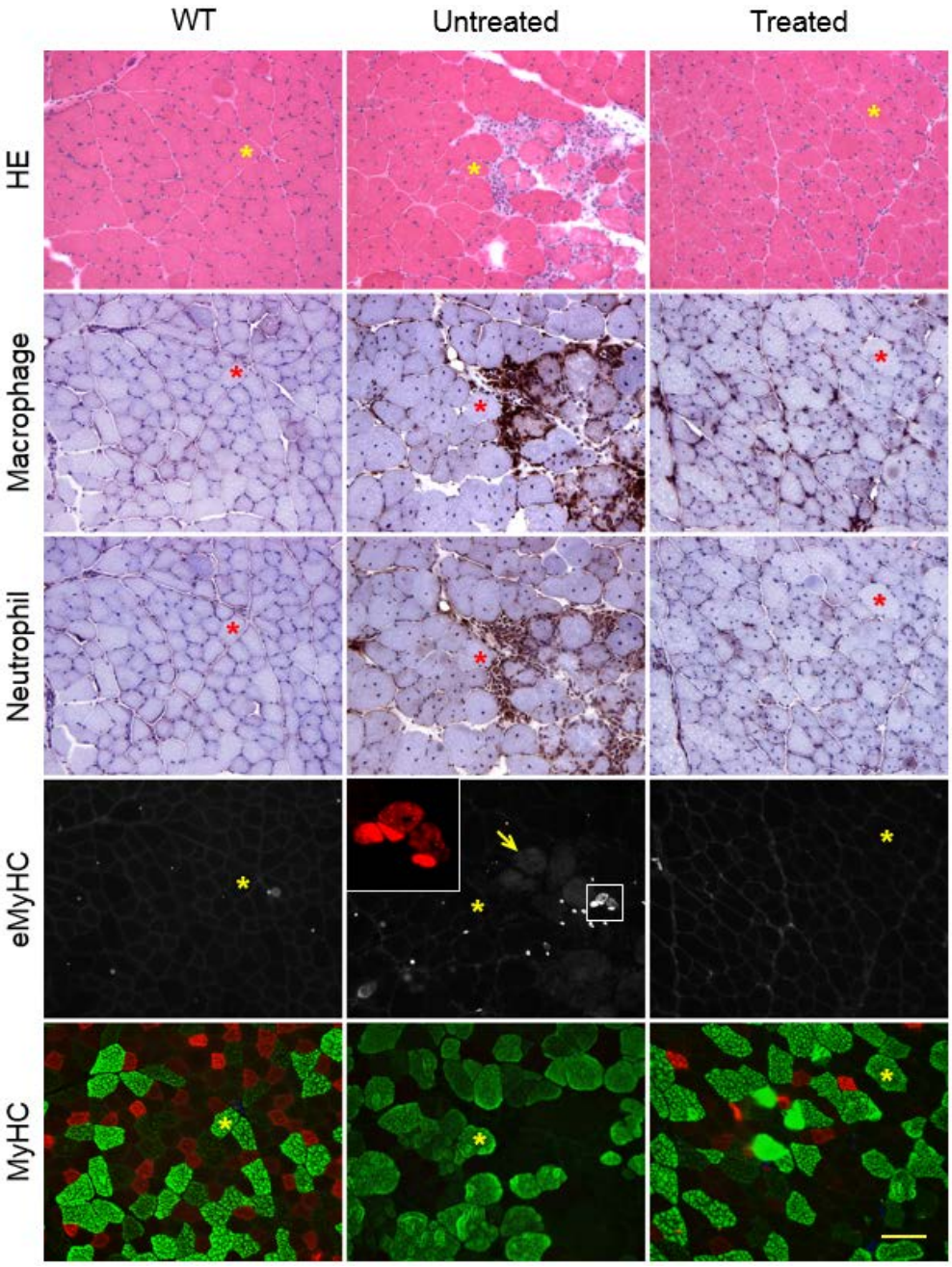

Fig. S11.

Representative photomicrographs of H&E staining, macrophage and neutrophil immunohistochemical staining, and myofiber type immunofluorescence staining. eMyHC, embryonic myosin heavy chain. **MyHC,** myosin heavy chain**.** Insert in the eMHC panel is an enlarged view of the boxed region in the same panel. For MHC staining, blue marks type I fiber. Red marks type IIA fiber. Green marks type IIB fiber and black marks type IIx fiber. **Arrow,** Strong cytosolic staining reflecting accumulation of mouse immunoglobulin (IgG) in damaged myofibers. IgG reacts with the fluorescein-conjugated mouse anti-mouse antibody (secondary antibody). **Asterisk,** the same myofiber in serial sections. **Scale bar,** 100 μm.

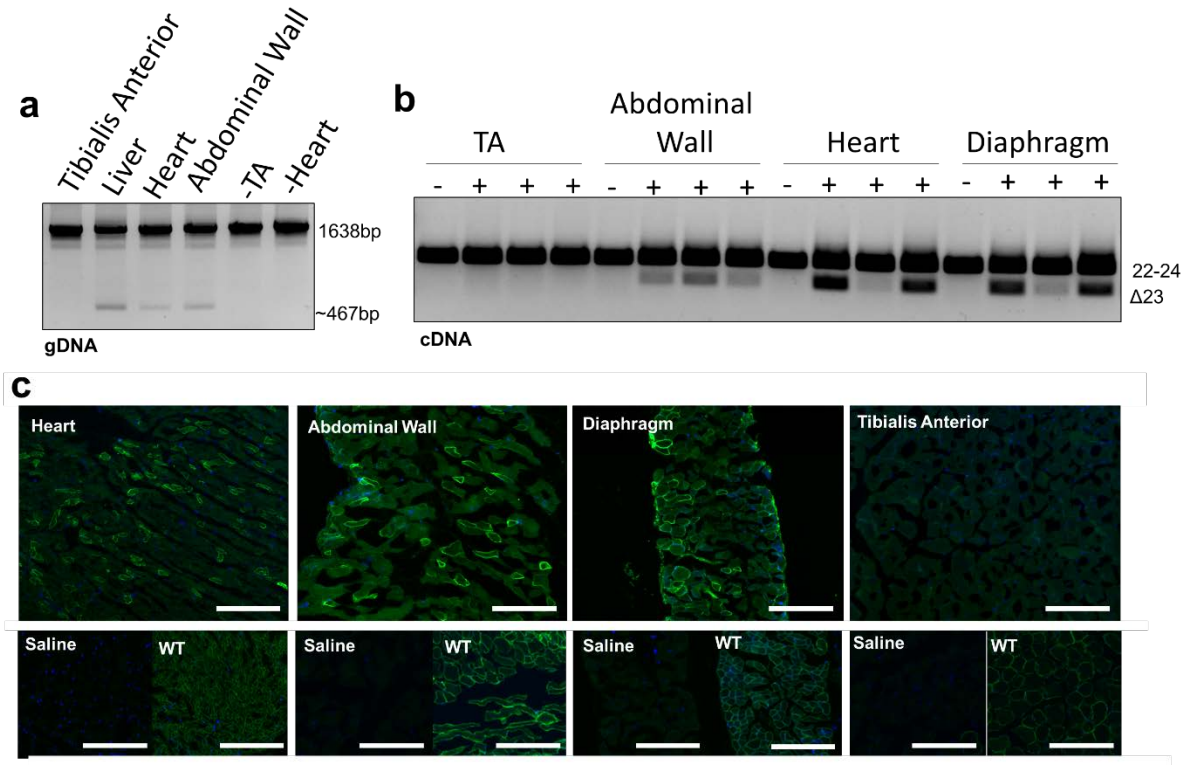

Fig. S12.

Systemic administration of CRISPR/Cas9 by intraperitoneal injection of AAV vectors recovers dystrophin in cardiac and skeletal muscles. (a) PCR across the genomic deletion shows removal of exon 23 from the genomic DNA in the liver, heart, and abdominal wall. (b) Removal of exon 23 from the mRNA transcript is shown strongly in the abdominal wall, heart, and diaphragm but not in distal muscles including the tibialis anterior. (c) Immunofluorescence staining of whole muscle sections shows abundant dystrophin expression in the heart, abdominal wall, and diaphragm. Distal muscles including the tibialis anterior (shown) were not significantly corrected. Scale bar = 200 μm.

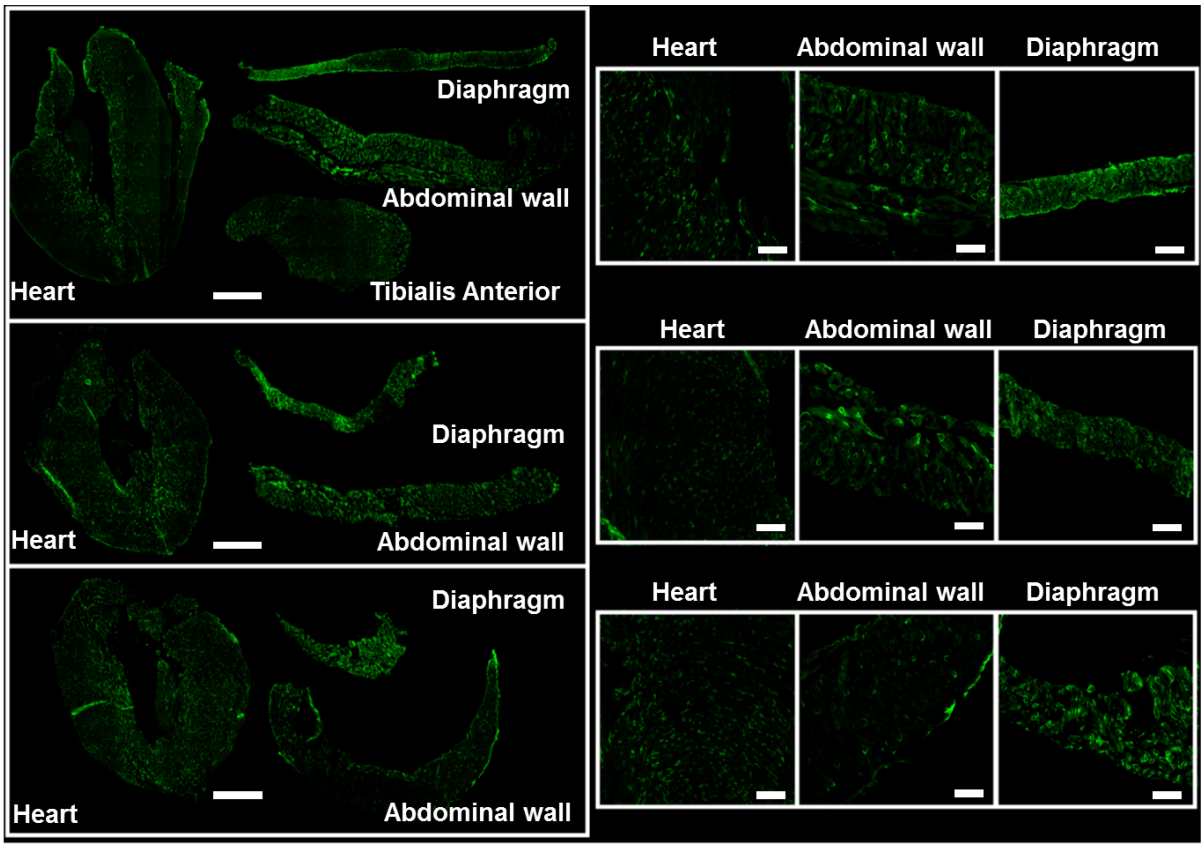

Fig. S13.

Full data panel for immunostaining for dystrophin from intraperitoneal administrated P2 neonates. Stained sections of heart, diaphragm, and abdominal wall muscles are shown from three independent mice. Left panels, full-view images (scale bar: 1 mm). Right panels, high power images (scale bar: 200 μm).

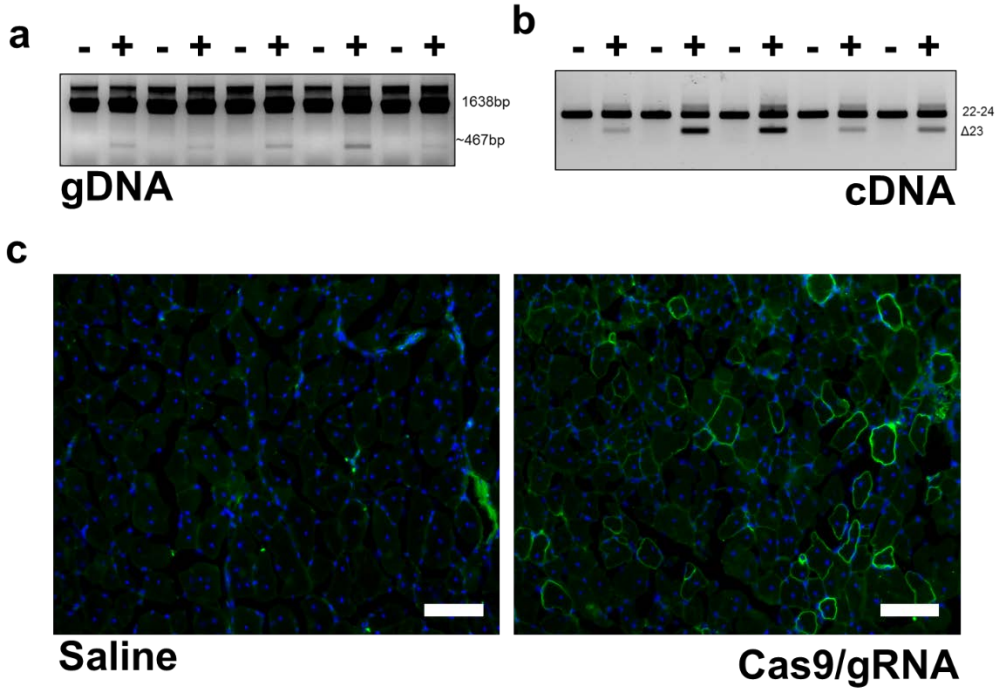

Fig. S14.

Genome editing is preserved for 6 months after a single injection of AAV-CRISPR. (a) Genomic DNA maintains the 1171bp deletion containing exon 23 (b) RT-PCR shows preservation of the Δ23 transcript. (c) Immunoflourescence staining of dystrophin shows preservation of restored dystrophin protein. Scale bar: 100 μm.

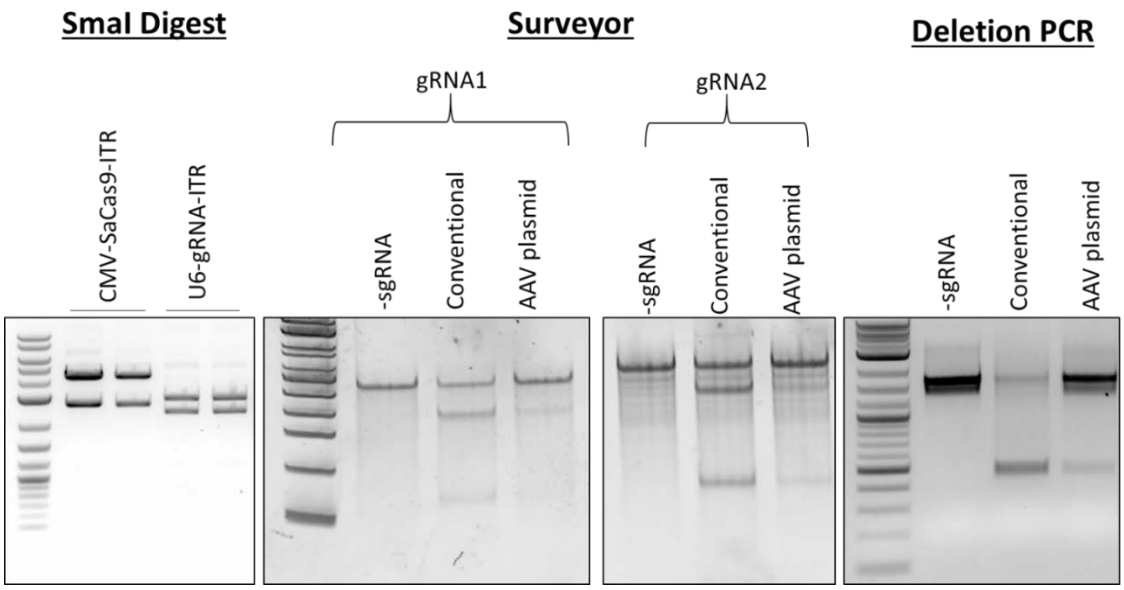

Fig. S15.

AAV transfer plasmid preparation. SmaI digestion indicates intact ITRs in preparation for AAV production. Surveyor and deletion PCR from mouse myoblasts using plasmids with ITRS (AAV plasmid) or without (conventional) shows slight reduction in Cas9 activity between plasmid architecture.

From Fig 1b

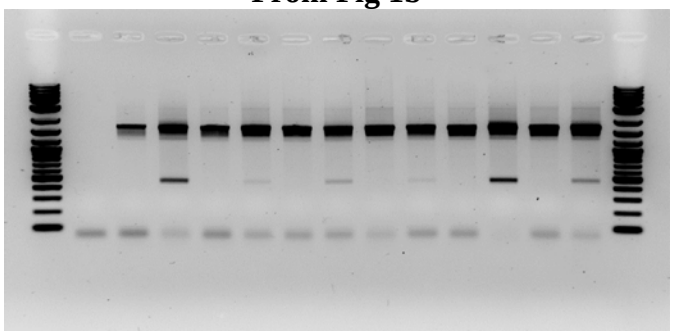

From Fig. 4a

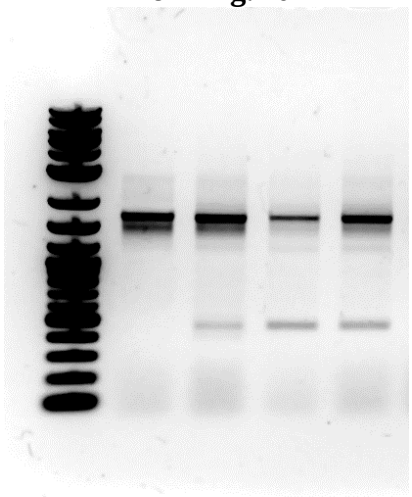

Fig. S16.

Full gel image from Fig. 1b and 4a. Genomic deletion represented by a 1638 bp parent band and a 467 bp deletion product.

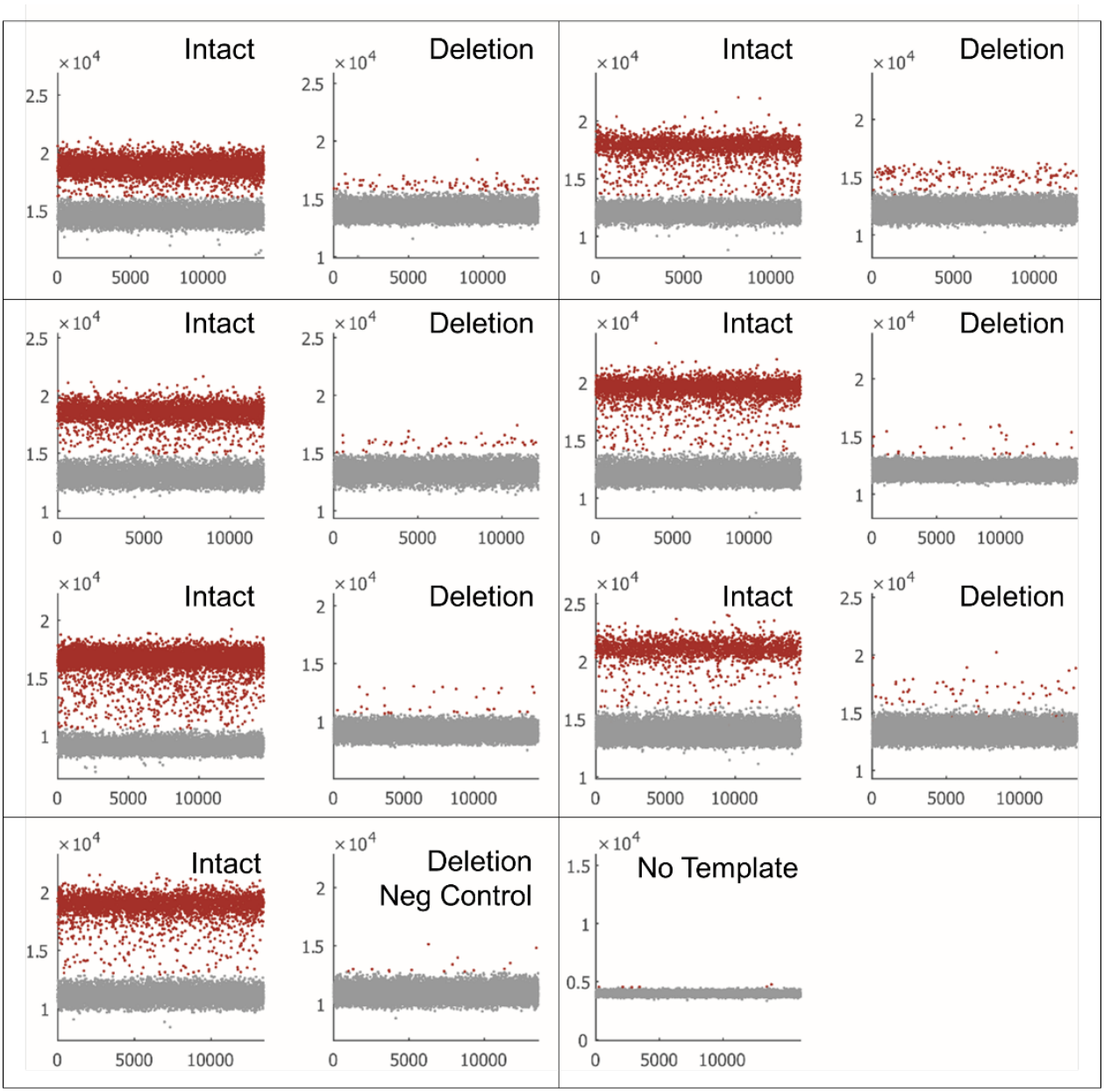

Fig. S17.

Complete ddPCR gDNA data panel from Fig. 1c. ddPCR for genomic DNA in 6 treated mice with primers specific for the intact dystrophin gene or the dystrophin gene missing the exon 23 region.

From Fig 1d

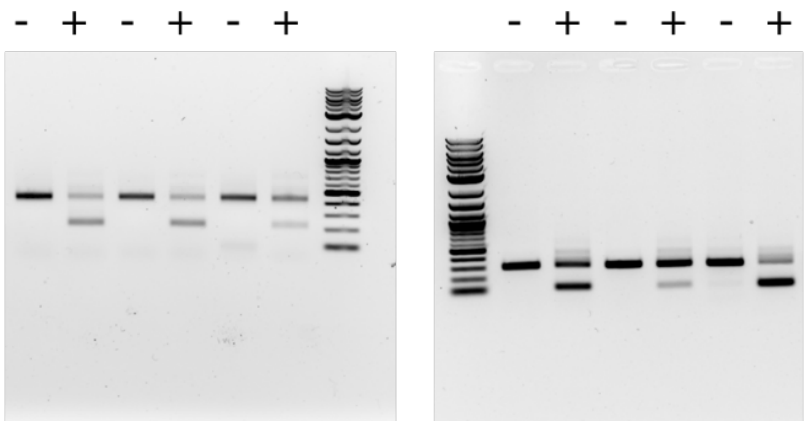

From Fig 4b

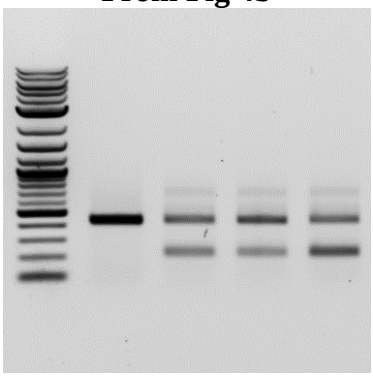

Fig. S18.

Full gels From Fig. 1d. Exon 23 was removed from the transcript of mice treated with Cas9/gRNAs as indicated by the smaller band.

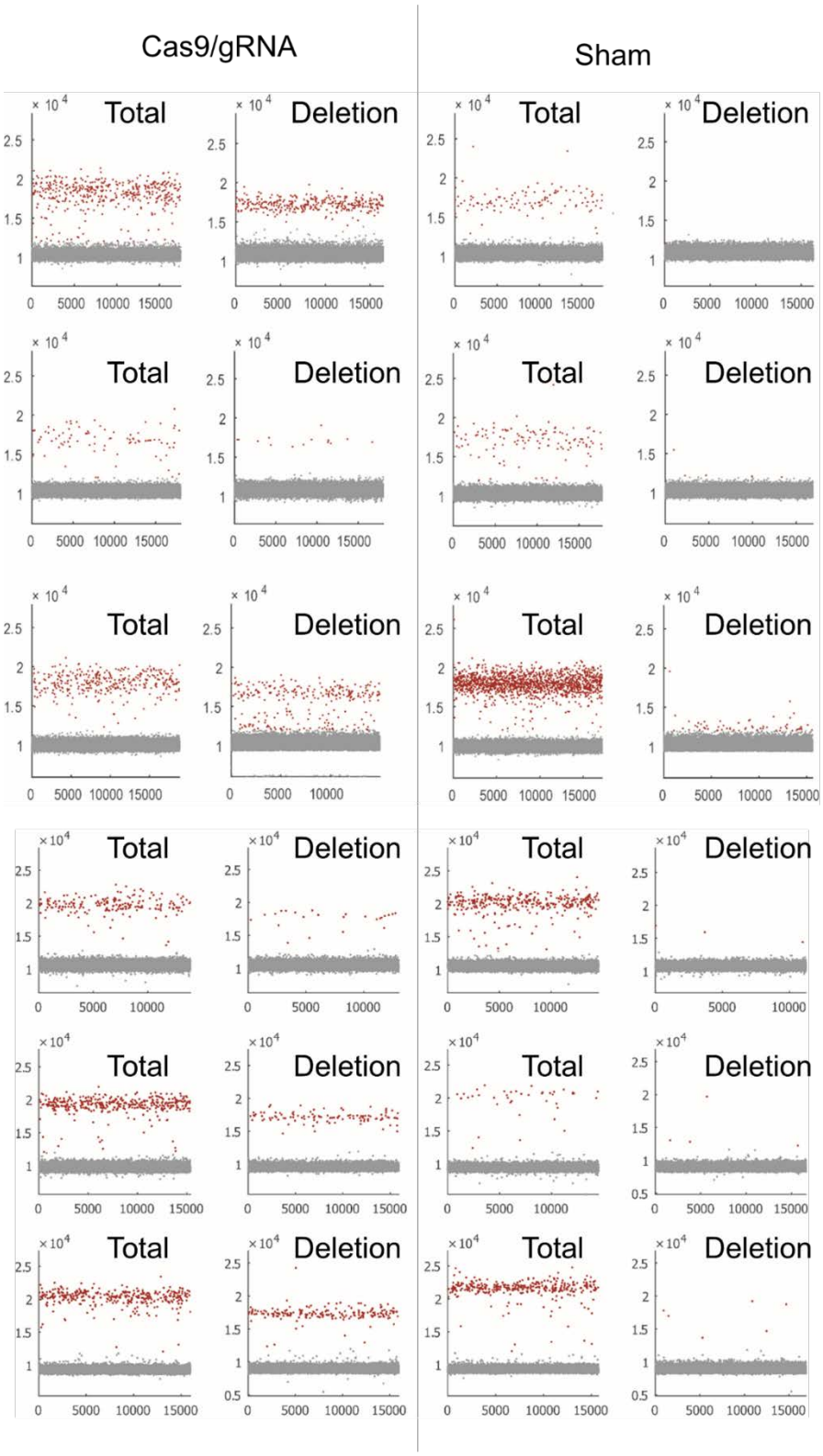

Fig. S19.

Complete ddPCR panel for dystrophin cDNA from Fig. 1e. Complete ddPCR data showing the deletion product relative to total dystrophin RNA expression.

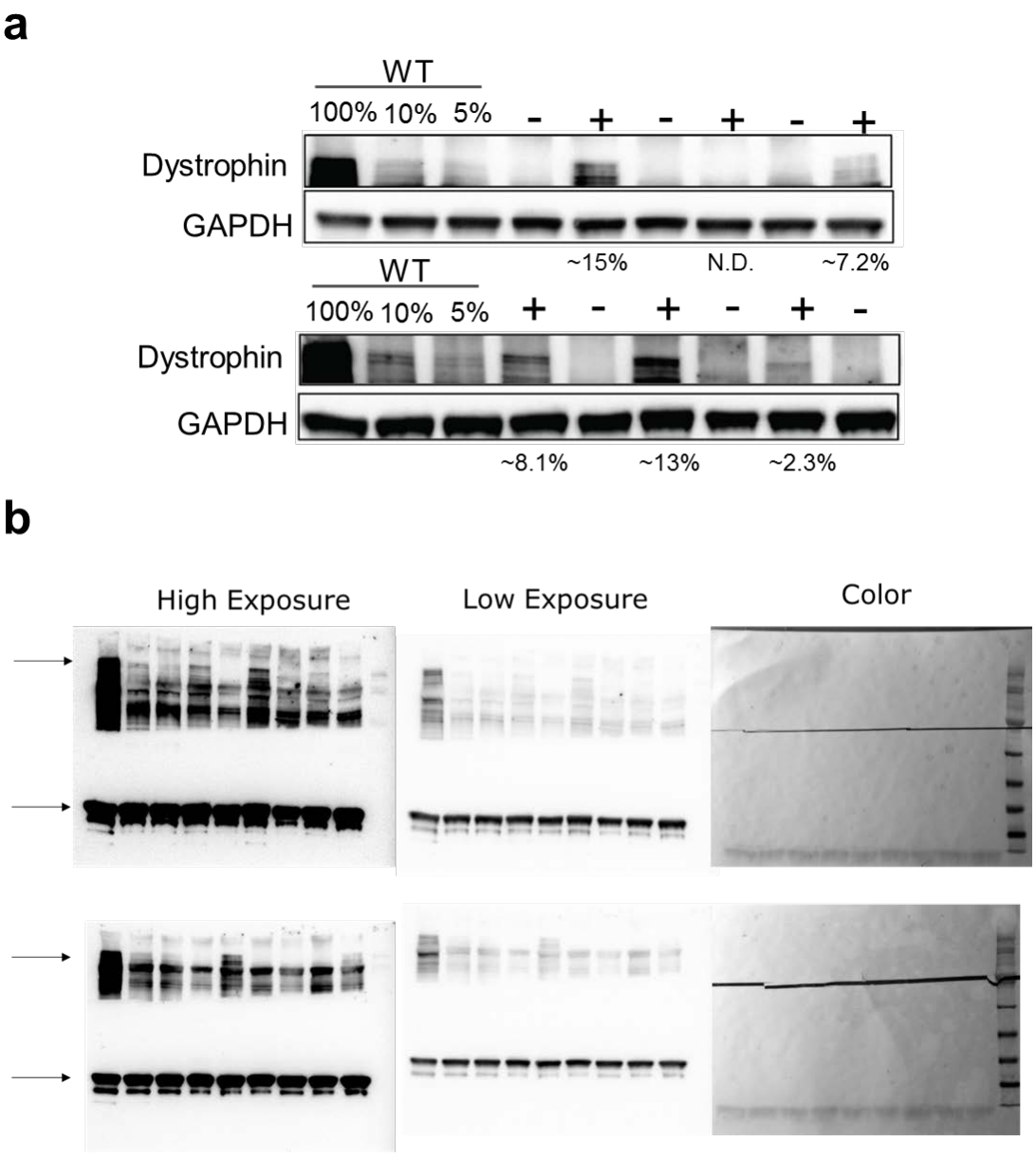

Fig. S20.

(a) Representative dystrophin western blot using the Mandys-8 antibody. (b) High and low exposure full blots are shown with arrows marking dystrophin and GAPDH expected protein sizes.

Cas9/gRNA-treated mice

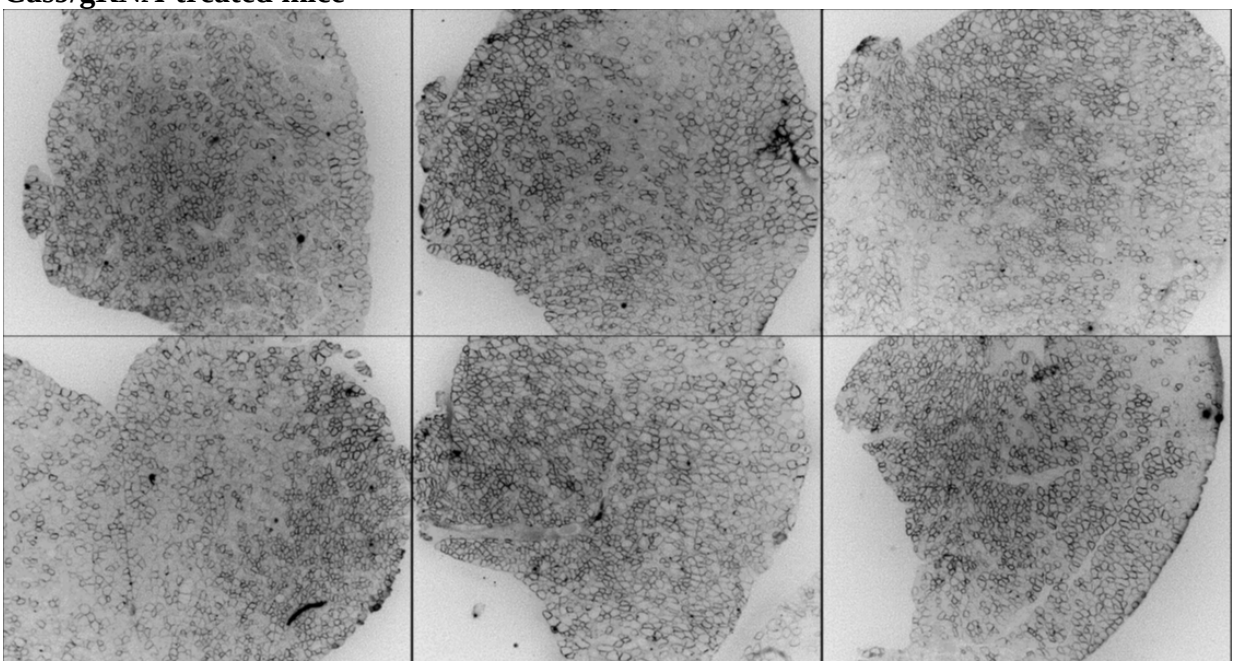

Sham injected mice

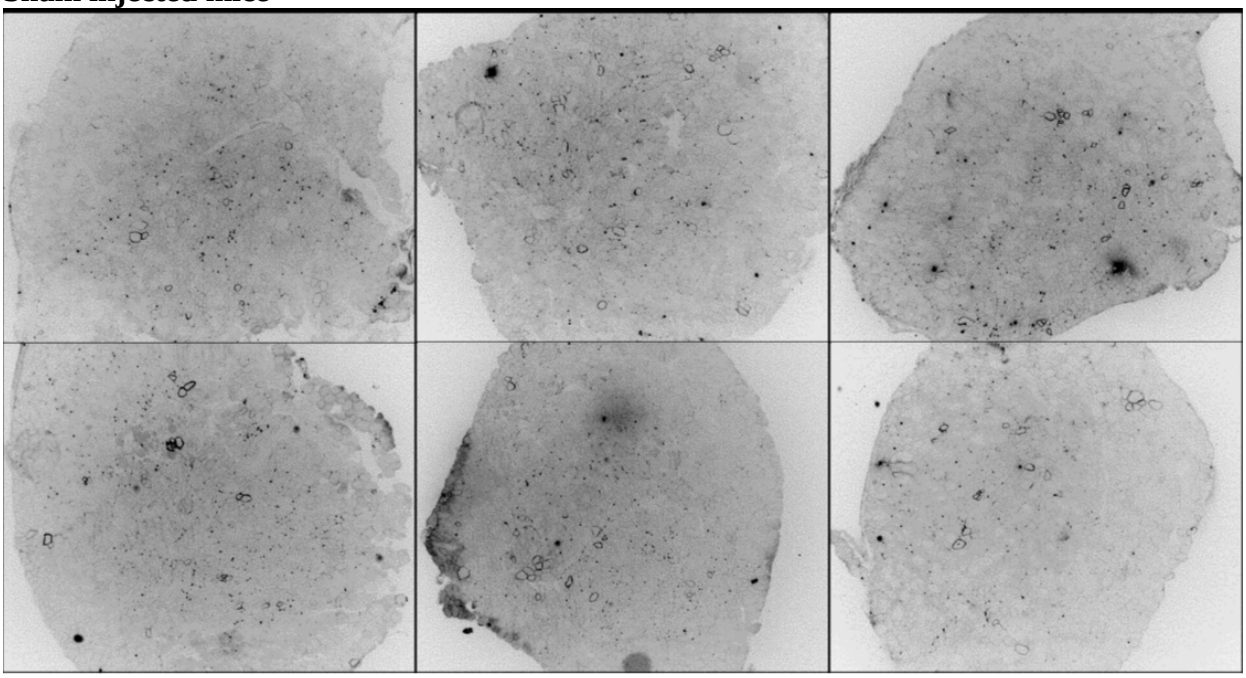

Fig. S21.

Representative photomicrographs of dystrophin stained muscle sections from CRISPR/gRNA treated muscles (top two rows) and sham injected muscles (bottom two rows).

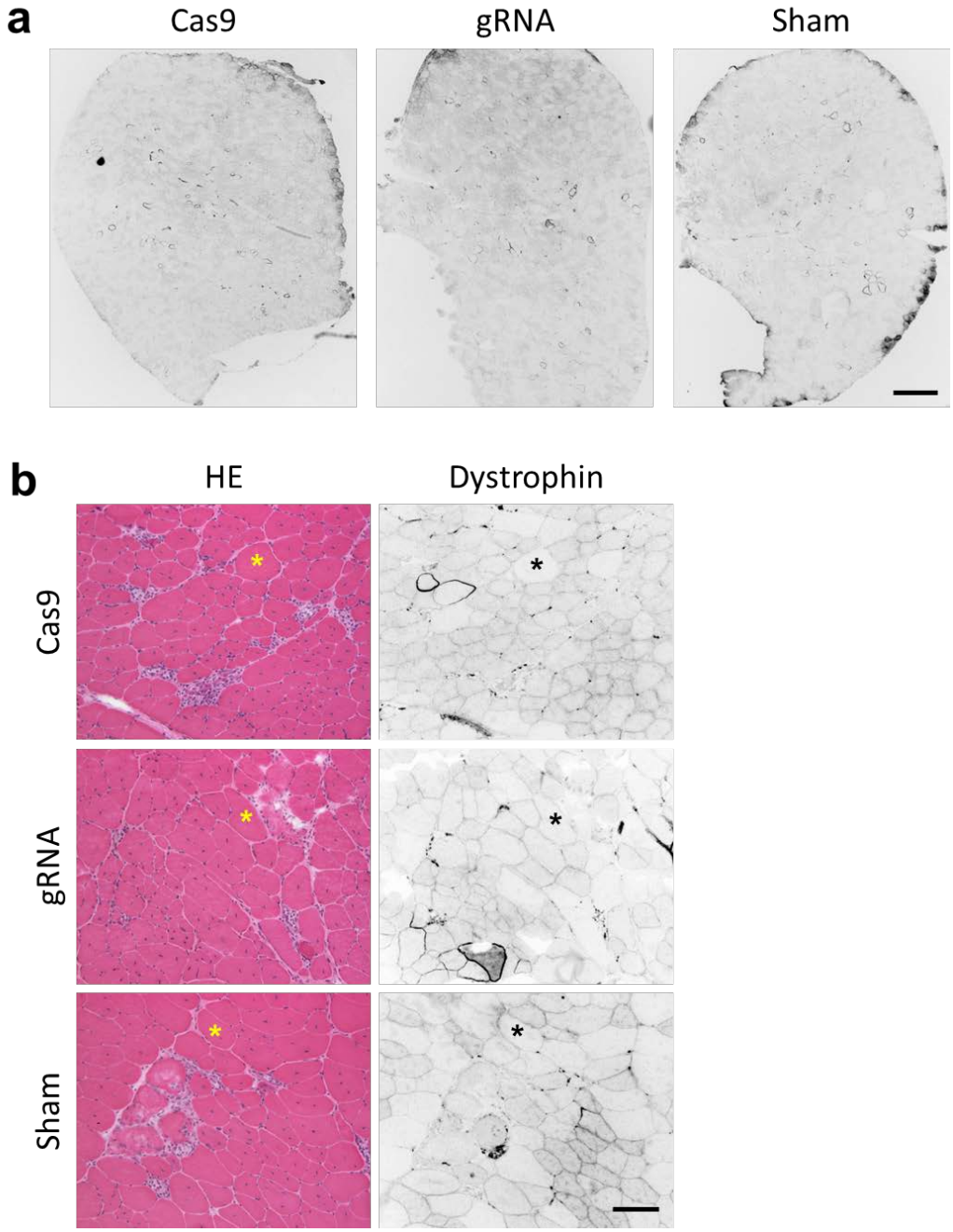

Fig. S22.

Injection of AAV.Cas9 or AAV.gRNA alone did not restore dystrophin expression. (a) Representative full-view dystrophin immunostaining of the tibialis anterior muscle that received either Cas9 or gRNA AAV vector. (b) Representative H&E and dystrophin immunostaining photomicrographs revealing no improvement in histology following single vector injection. Scale bar = 500 μm for panel a; scale bar = 100 μm for panel b.

Table S1.

Primer List

Name	Sequence	Description
BbsI/Guide RNA cloning primers		
gRNA01-S	CACCGTACACTAACACGCATATTTG	Sense Primer for gRNA1
gRNA01-AS	AAACCAAATATGCGTGTTAGTGTAC	Antisense Primer for gRNA1
gRNA02-S	CACCGCATTGCATCCATGTCTGACT	Sense Primer for gRNA2
gRNA02-AS	AAACAGTCAGACATGGATGCAATGC	Antisense Primer for gRNA2
gRNA03-S	CACCGAATTACAGGTCTGTGGACAT	Sense Primer for gRNA3
gRNA03-AS	AAACATGTCCACAGACCTGTAATTC	Antisense Primer for gRNA3
gRNA04-S	CACCGTTTAAGCTTAGGTAAAATCA	Sense Primer for gRNA4
gRNA04-AS	AAACTGATTTTACCTAAGCTTAAAC	Antisense Primer for gRNA4
gRNA05-S	CACCGATTTAGAGATCTAAACAAAG	Sense Primer for gRNA5
gRNA05-AS	AAACCTTTGTTTAGATCTCTAAATC	Antisense Primer for gRNA5
gRNA06-S	CACCGTGGGAAACAGATATTTTACC	Sense Primer for gRNA6
gRNA06-AS	AAACGGTAAAATATCTGTTTCCCAC	Antisense Primer for gRNA6
gRNA07-S	CACCGCAAAAGCCAAATCTATTTCA	Sense Primer for gRNA7
gRNA07-AS	AAACTGAAATAGATTTGGCTTTTGC	Antisense Primer for gRNA7
gRNA08-S	CACCGCAGTAATGTGTCATACCTTC	Sense Primer for gRNA8
gRNA08-AS	AAACGAAGGTATGACACATTACTGC	Antisense Primer for gRNA8
gRNA09-S	CACCGTTCTTGGATTGTCTGTATAA	Sense Primer for gRNA9
gRNA09-AS	AAACTTATACAGACAATCCAAGAAC	Antisense Primer for gRNA9
gRNA10-S	CACCGAAAAATGTCATGACTTCATA	Sense Primer for gRNA10
gRNA10-AS	AAACTATGAAGTCATGACATTTTTC	Antisense Primer for gRNA10
gRNA11-S	CACCGTTCACTACCATATTTCACTT	Sense Primer for gRNA11
gRNA11-AS	AAACAAGTGAAATATGGTAGTGAAC	Antisense Primer for gRNA11
gRNA12-S	CACCGCCATATTTCACTTTTGAATT	Sense Primer for gRNA12
gRNA12-AS	AAACAATTCAAAAGTGAAATATGGC	Antisense Primer for gRNA12
gRNA13-S	CACCGGATCAAGTCACTAGCATGGC	Sense Primer for gRNA13
gRNA13-AS	AAACGCCATGCTAGTGACTTGATCC	Antisense Primer for gRNA13
gRNA14-S	CACCGAAACAGATTCAGAGTCAGAC	Sense Primer for gRNA14
gRNA14-AS	AAACGTCTGACTCTGAATCTGTTTC	Antisense Primer for gRNA14

AAV transfer plasmid cloning primers		
F-AAV-gRNA1	GTGGTGGGTACCagatctaggaaCCTAGGgcctatt tcccatgattccttc	pTR-EGFP-SaCas9-sgRNA1-F Subclone 1st SaCas9 sgRNA with KpnI/XbaI into pTR-eGFP
R-AAV-gRNA1	CACCACTCTAGAattaaccctcactaaaggga	pTR-EGFP-SaCas9-sgRNA1-R Subclone 1st SaCas9 sgRNA with KpnI/XbaI into pTR-eGFP
F-AAV-gRNA2	GTGGTGGGTACCgcctatttcccatgattccttc	pTR-EGFP-SaCas9-sgRNA2-F Subclone 2nd SaCas9 sgRNA with KpnI/AvrII into pTR-eGFP

R-AAV-gRNA1	GTGGTGCCTAGGattaaccctcactaaaggga	pTR-EGFP-SaCas9-sgRNA2-R Subclone 2nd SaCas9 sgRNA with KpnI/AvrII into pTR-eGFP

Surveyor/qPCR primers		
In22-gRNA1/6-F	tttgttgattctaaaaatcccatgt	Surveyor Primers for gRNA1, gRNA5
In22-gRNA1/6-R	atatttctgaaggtgctttcttgg	Rev-Survyor Primers for gRNA1 gRNA5
In23-gRNA2/13/14-F	gtgtttctcatagttggccatttg	FwdSurveyor Primers for gRNA2, gRNA13, gRNA14
In23-gRNA2/13/14-R	Ggactgaagaacttggagaagga	Rev- Surveyor Primers for gRNA2, gRNA13, gRNA14
In22-gRNA3-F	TCCAGCAGTCAGAAAGCAAA	Surveyor Primers for gRNA3
In22-gRNA3-R	TGTTTTTGGTCAAATTGTTCTGTT	Surveyor Primers for gRNA3
In22-gRNA4-F	GAACAATTTGACCAAAAACATGA	Surveyor Primers for gRNA4
In22-gRNA4-R	TGTCCTCACATCACAGAAGTTT	Surveyor Primers for gRNA4
dPCR-intact-F	TCATAGTTGGCCATTTGTGAAA	Fwd Primer gDNA dPCR intact dystrophin
dPCR-R	GGTACAGTGTTAGGGAGCAGGA	Rev Primer gDNA dPCR
dPCR-del-F	TTTCTGTCTAAATATAATATGCCCTGT	Fwd Primer gDNA dPCR deleted dystrophin
dPCR-ex22-F	ggatccagcagtcagaaagc	Fwd Primer cDNA dPCR binds exon 22
dPCR-ex22/24-F	ctcgggaaattacagaatcaca	Fwd Primer cDNA dPCR binds exon22-24 junction
dPCR-ex24/25-R	tcaccaactaaaagtctgcattg	Rev Primer cDNA dPCR binds exon 24-25 junction

Miseq primers		
In22-Miseq-F	TCGTCGGCAGCGTCAGATGTGTATAAGAGACAGtttctgtctaaatataatatgccctgt	chrX:83803255
In22-Miseq-R	GTCTCGTGGGCTCGGAGATGTGTATAAGAGACAGgcagagcctcaaaattaaatagaag	
In22-Miseq-OT1F	TCGTCGGCAGCGTCAGATGTGTATAAGAGACAGaatgttcttggagccaatttgt	chr14:38227244
In22-Miseq-OT1R	GTCTCGTGGGCTCGGAGATGTGTATAAGAGACAGagcttcaacattctccaacca	
In22-Miseq-OT2F	TCGTCGGCAGCGTCAGATGTGTATAAGAGACAGatcgacagacagatacacatcca	chr6:37580259
In22-Miseq-OT2R	GTCTCGTGGGCTCGGAGATGTGTATAAGAGACAGaaaatggttgaagccagctc	
In22-Miseq-OT3F	TCGTCGGCAGCGTCAGATGTGTATAAGAGACAGttgaaaggttttgctgggata	chrX:93621693
In22-Miseq-OT3R	GTCTCGTGGGCTCGGAGATGTGTATAAGAGACAGaggaacaatgctccaaccac	
In22-Miseq-OT4F	TCGTCGGCAGCGTCAGATGTGTATAAGAGACAGctgcttgtgcctgctgtaaa	chr10:17880418
In22-Miseq-OT4R	GTCTCGTGGGCTCGGAGATGTGTATAAGAGACAGccgtgttttggtgtctagga	
In22-Miseq-OT5F	TCGTCGGCAGCGTCAGATGTGTATAAGAGACAGtattcttgtcaggcccaacc	chr13:68811666

In22-Miseq-OT5R	GTCTCGTGGGCTCGGAGATGTGTATAAGAGACAGttctgtgttggtgcttgctt	
In22-Miseq-OT6F	TCGTCGGCAGCGTCAGATGTGTATAAGAGACAGttcagccacataatctcagga	chr15:24587776
In22-Miseq-OT6R	GTCTCGTGGGCTCGGAGATGTGTATAAGAGACAGccatatctatatctatatccacacacc	
In22-Miseq-OT7F	TCGTCGGCAGCGTCAGATGTGTATAAGAGACAGgcttagtagcagaaattgggaaa	chr17:61598639
In22-Miseq-OT7R	GTCTCGTGGGCTCGGAGATGTGTATAAGAGACAGtttgccgttgtattttatgttg	
In22-Miseq-OT8F	TCGTCGGCAGCGTCAGATGTGTATAAGAGACAGaaagttgttagagcctgctcatt	chr19:58691040
In22-Miseq-OT8R	GTCTCGTGGGCTCGGAGATGTGTATAAGAGACAGtttagtagacggaagaaagctca	
In22-Miseq-OT9F	TCGTCGGCAGCGTCAGATGTGTATAAGAGACAGttggaagcataattatagatacctgaa	chr3:75338035
In22-Miseq-OT9R	GTCTCGTGGGCTCGGAGATGTGTATAAGAGACAGaattggcagaagctggactg	
In22-Miseq-OT10F	TCGTCGGCAGCGTCAGATGTGTATAAGAGACAGtttcatgcagaatgggtgag	chr4:74219376
In22-Miseq-OT10R	GTCTCGTGGGCTCGGAGATGTGTATAAGAGACAGatgcacacattcactgcaca	
In23-Miseq-F	TCGTCGGCAGCGTCAGATGTGTATAAGAGACAGgagctcatcctctttcatgct	chrX:83804418
In23-Miseq-R	GTCTCGTGGGCTCGGAGATGTGTATAAGAGACAGgaaggaggaacaggcaggag	
In23-Miseq-OT11F	TCGTCGGCAGCGTCAGATGTGTATAAGAGACAGaacccttctgtctcagcctc	chr11:79174648
In23-Miseq-OT11R	GTCTCGTGGGCTCGGAGATGTGTATAAGAGACAGggttcctttgccccatgaag	
In23-Miseq-OT12F	TCGTCGGCAGCGTCAGATGTGTATAAGAGACAGgcacctgggcttggaatttt	chr14:44650592
In23-Miseq-OT12R	GTCTCGTGGGCTCGGAGATGTGTATAAGAGACAGccacatggttttctaggttgttc	
In23-Miseq-OT13F	TCGTCGGCAGCGTCAGATGTGTATAAGAGACAGtggtgataaacagcagca	chr16:52827780
In23-Miseq-OT13R	GTCTCGTGGGCTCGGAGATGTGTATAAGAGACAGcagccatacccagggatcta	
In23-Miseq-OT14F	TCGTCGGCAGCGTCAGATGTGTATAAGAGACAGagtacaccaagctccatccc	chr4:65302210
In23-Miseq-OT14R	GTCTCGTGGGCTCGGAGATGTGTATAAGAGACAGggtgggaggattgggattca	
In23-Miseq-OT15F	TCGTCGGCAGCGTCAGATGTGTATAAGAGACAGtgtgtgctttagggtttctgg	chr6:63142428
In23-Miseq-OT15R	GTCTCGTGGGCTCGGAGATGTGTATAAGAGACAGcttctgcagtgctctttgga	
In23-Miseq-OT16F	TCGTCGGCAGCGTCAGATGTGTATAAGAGACAGcacagttcatgcaatgtggga	chrX:126550272
In23-Miseq-OT16R	GTCTCGTGGGCTCGGAGATGTGTATAAGAGACAGatgtctctgtgctggtcctc	
In23-Miseq-OT17F	TCGTCGGCAGCGTCAGATGTGTATAAGAGACAGacgggacctcataaaattgc	chr3:99899506
In23-Miseq-OT17R	GTCTCGTGGGCTCGGAGATGTGTATAAGAGACAGcagtcattcggtattcctcg	
In23-Miseq-OT18F	TCGTCGGCAGCGTCAGATGTGTATAAGAGACAGtggatatcctcctgggaatg	chrX:122567507
In23-Miseq-OT18R	GTCTCGTGGGCTCGGAGATGTGTATAAGAGACAGgcctcaactggaaactgagc	
In23-Miseq-OT19F	TCGTCGGCAGCGTCAGATGTGTATAAGAGACAGcttggtgaccacccaagtct	chr2:38535351
In23-Miseq-OT19R	GTCTCGTGGGCTCGGAGATGTGTATAAGAGACAGactgccattcatgtgtccaa	
In232-Miseq-OT20F	TCGTCGGCAGCGTCAGATGTGTATAAGAGACAGgccaccaactcccagataaa	chr4:8499023
In23-Miseq-OT20R	GTCTCGTGGGCTCGGAGATGTGTATAAGAGACAGcttgaaatttgccctggttc	
Nested PCR primers for miSEQ with barcodes underlined		
Universal i5 primer	AATGATACGGCGACCACCGAGATCTACACTCGTCGGCAGCGTC	
BC1	CAAGCAGAAGACGGCATACGAGAT**ACATCG**GTCTCGTGGGCTCGG	
BC2	CAAGCAGAAGACGGCATACGAGAT**TGGTCA**GTCTCGTGGGCTCGG	
BC3	CAAGCAGAAGACGGCATACGAGAT**CACTGT**GTCTCGTGGGCTCGG	

BC4	CAAGCAGAAGACGGCATACGAGAT**ATTGGC**GTCTCGTGGGCTCGG	
BC5	CAAGCAGAAGACGGCATACGAGAT**GATCTG**GTCTCGTGGGCTCGG	
BC6	CAAGCAGAAGACGGCATACGAGAT**TACAAG**GTCTCGTGGGCTCGG	
BC7	CAAGCAGAAGACGGCATACGAGAT**CGTGAT**GTCTCGTGGGCTCGG	
BC8	CAAGCAGAAGACGGCATACGAGAT**GCCTAA**GTCTCGTGGGCTCGG	
BC9	CAAGCAGAAGACGGCATACGAGAT**TCAAGT**GTCTCGTGGGCTCGG	
BC10	CAAGCAGAAGACGGCATACGAGAT**AGCTAG**GTCTCGTGGGCTCGG	
BC11	CAAGCAGAAGACGGCATACGAGAT**GTCGTC**GTCTCGTGGGCTCGG	
BC12	CAAGCAGAAGACGGCATACGAGAT**CGATTA**GTCTCGTGGGCTCGG	
BC13	CAAGCAGAAGACGGCATACGAGAT**GAATGA**GTCTCGTGGGCTCGG	
BC14	CAAGCAGAAGACGGCATACGAGAT**CTTCGA**GTCTCGTGGGCTCGG	
BC15	CAAGCAGAAGACGGCATACGAGAT**CTCTAC**GTCTCGTGGGCTCGG	
BC16	CAAGCAGAAGACGGCATACGAGAT**AGGAAT**GTCTCGTGGGCTCGG	
BC17	CAAGCAGAAGACGGCATACGAGAT**GCTACC**GTCTCGTGGGCTCGG	
BC18	CAAGCAGAAGACGGCATACGAGAT**ATCAGT**GTCTCGTGGGCTCGG	

Table S2.

Summary of indel formation within the target cut site and the top 10 off target sites. Three target sites (gRNA1-OT10, gRNA-OT2, gRNA2-OT7) did not meet filtering criteria

	#	Sequence	PAM	Chr	Gene	#MM	%Indels	Treated/ Untreated
gRNA1-Intron22	**On**	**TACACTAACACGCATATTTG**	**ATGAGT**	**chrX**	**DMD-intron22**	**0**	**2.49% (± 0.96%)**	**12.84**
	OT1	TACACacACAtGCATATTTG	GTGGAT	chr14	None	3	0.63% (± 0.01%)	0.98
	OT2	TACACatACACaCATATTTG	GTGGAT	chr6	5' of : Gm25062-201 ENSMUST00000104660	3	0.12% (± 0.00%)	1.02
	OT3	TACACTtACACaCATAgTTG	ATGGAT	chrX	Intron 3 of MGI:99660, ENSMUSG000000006678	3	0.32% (± 0.02%)	1.27
	OT4	TgCACTAtaAaGCATATTTG	AAGGAT	chr10	None	4	0.10% (± 0.01%)	1.05
	OT5	cACACacACACaCATATTTG	GTGGAT	chr13	Intron 3 of Adcy2-201	4	1.23% (± 0.03%)	1.07
	OT6	cACACccACACaCATATTTG	GAGGGT	chr15	None	4	1.28% (± 0.05%)	0.97
	OT7	TgCttgAACACGCATATTTG	AGGAAT	chr17	None	4	0.15% (± 0.01%)	1.01
	OT8	**TACAtatACACaCATATTTG**	**GTGGAT**	**chr19**	**Intron 4 of Y1G0141A14**	**4**	**1.01% (± 0.33%)**	**6.66**
	OT9	TAaAgTAACcCaCATATTTG	GTGGAT	chr3	None	4	0.11% (± 0.01%)	0.97
	OT10	cACACacACACaCATATTTG	GTGGAT	chr4	None	4	N/A	N/A
gRNA2-Intron23	**On**	**CATTGCATCCATGTCTGACT**	**CTGAAT**	**chrX**	**DMD-intron23**	**0**	**3.12% (± 1.01%)**	**84.04**
	OT1	gAcTGCcTCCATGTCTGACT	GAGGAT	chr11	None	3	0.06% (± 0.00%)	0.91
	OT2	CATTGCAgCaATGTCTGAaT	CTGAGT	chr14	Intron 4 of NSMUST000000169583	3	N/A	N/A
	OT3	CATTGCATaCATGTCTtAgT	CAGGGT	chr16	Intron 2 of Mbi-105	3	0.12% (± 0.01%)	0.95
	OT4	CATTtCATCCAgGTCTtACT	TAGAAT	chr4	Intron 13 of Pappa	3	0.15% (± 0.01%)	1.09
	OT5	CATTtCATtCATGTCTGACa	TGGAGT	chr6	None	3	0.06% (± 0.01%)	1.12
	OT6	CATTGCATCCAaGTgTGACc	CTGAAT	chrX	None	3	0.11% (± 0.01%)	0.92
	OT7	tATTaatTCCATGTCTGACT	TAGGAT	chr3	Intron 1 of Spag17	4	N/A	N/A
	OT8	ggcTcCATCCATGTCTGACT	TAGGGT	chrX	None	4	0.09% (± 0.01%)	0.99
	OT9	CAgaGCAgCtATGTCTGACT	ATGAAT	chr2	Intron 1 Nek6	4	0.09% (± 0.00%)	1.22
	OT10	gATgcCATCCATGaCTGACT	CAGAAT	chr4	None	4	0.14% (± 0.01%)	1.30

Table S3.

Detailed summary of deep sequencing of target sequence and top 10 off-target sequences for each guide RNA.

Control						Treated					
gRNA1-Intron22						**gRNA1-Intron22**					
	%Indels	Total Reads	Deletion	Insertions	Mismatch	%Indels	Total Reads	Deletion	Insertions	Mismatch
ON	**0.23% (± 0.19%)**	**21959 (± 1804)**	**0.17% (± 0.01%)**	**0.14% (± 0.01%)**	**2.83% (± 0.02%)**	**2.49% (± 0.96%)**	**20172 (± 22493)**	**2.14% (± 0.82%)**	**0.45% (± 0.14%)**	**2.73% (± 0.11%)**
OT1	0.66% (± 0.64%)	22198 (± 2145)	0.62% (± 0.01%)	0.06% (± 0.01%)	2.62% (± 0.07%)	0.63% (± 0.01%)	22529 (± 22400)	0.62% (± 0.01%)	0.05% (± 0.01%)	2.66% (± 0.09%)
OT2	0.14% (± 0.12%)	25839 (± 3479)	0.10% (± 0.01%)	0.09% (± 0.01%)	6.94% (± 0.14%)	0.12% (± 0.00%)	29029 (± 30473)	0.11% (± 0.01%)	0.08% (± 0.01%)	7.04% (± 0.05%)
OT3	0.32% (± 0.25%)	20112 (± 1062)	0.23% (± 0.02%)	0.12% (± 0.01%)	3.38% (± 0.13%)	0.32% (± 0.02%)	13851 (± 18433)	0.30% (± 0.01%)	0.12% (± 0.01%)	3.38% (± 0.11%)
OT4	0.10% (± 0.10%)	26708 (± 2041)	0.09% (± 0.01%)	0.04% (± 0.00%)	2.05% (± 0.06%)	0.10% (± 0.01%)	17281 (± 20171)	0.09% (± 0.00%)	0.05% (± 0.01%)	2.13% (± 0.07%)
OT5	1.14% (± 1.14%)	27384 (± 1506)	1.03% (± 0.05%)	0.76% (± 0.05%)	7.66% (± 0.23%)	1.23% (± 0.03%)	16763 (± 19923)	1.08% (± 0.03%)	0.83% (± 0.04%)	7.73% (± 0.18%)
OT6	1.32% (± 1.32%)	23141 (± 1809)	1.29% (± 0.01%)	0.93% (± 0.03%)	35.50% (± 0.23%)	1.28% (± 0.05%)	20762 (± 21270)	1.25% (± 0.05%)	0.87% (± 0.03%)	35.37% (± 0.27%)
OT7	0.13% (± 0.15%)	40535 (± 5780)	0.13% (± 0.01%)	0.12% (± 0.01%)	2.67% (± 0.04%)	0.15% (± 0.01%)	25384 (± 27745)	0.13% (± 0.00%)	0.12% (± 0.01%)	2.69% (± 0.07%)
OT8	**0.15% (± 0.15%)**	**25575 (± 2362)**	**0.14% (± 0.01%)**	**0.09% (± 0.01%)**	**2.30% (± 0.04%)**	**1.01% (± 0.33%)**	**12177 (± 19961)**	**1.00% (± 0.33%)**	**0.09% (± 0.01%)**	**1.91% (± 0.08%)**
OT9	0.15% (± 0.11%)	20433 (± 4287)	1.13% (± 1.02%)	1.09% (± 1.03%)	4.66% (± 1.57%)	0.11% (± 0.01%)	9660 (± 21599)	0.10% (± 0.01%)	0.06% (± 0.01%)	2.99% (± 0.13%)
OT10	N/A	N/A	N/A	N/A	N/A	N/A	N/A	N/A	N/A	N/A

Control						Treated					
gRNA2-Intron23						**gRNA2-Intron23**					
	%Indels	Total Reads	Deletion	Insertions	Mismatch	%Indels	Total Reads	Deletion	Insertions	Mismatch
ON	**0.03% (± 0.04%)**	**24956 (± 1303)**	**0.03% (± 0.00%)**	**0.03% (± 0.00%)**	**2.30% (± 0.04%)**	**3.12% (± 1.01%)**	**23952 (± 2987)**	**2.77% (± 0.87%)**	**0.43% (± 0.17%)**	**2.33% (± 0.15%)**
OT1	0.05% (± 0.07%)	31700 (± 2393)	0.06% (± 0.01%)	0.03% (± 0.00%)	7.60% (± 0.13%)	0.06% (± 0.00%)	27636 (± 1441)	0.06% (± 0.00%)	0.03% (± 0.00%)	7.77% (± 0.06%)
OT2	N/A	N/A	N/A	N/A	N/A	N/A	N/A	N/A	N/A	N/A
OT3	0.14% (± 0.13%)	30882 (± 1343)	0.09% (± 0.00%)	0.09% (± 0.01%)	2.56% (± 0.08%)	0.12% (± 0.01%)	24231 (± 1068)	0.10% (± 0.01%)	0.08% (± 0.01%)	2.69% (± 0.07%)
OT4	0.12% (± 0.14%)	28762 (± 675)	0.12% (± 0.01%)	0.10% (± 0.01%)	4.07% (± 0.09%)	0.15% (± 0.01%)	24301 (± 1611)	0.14% (± 0.01%)	0.10% (± 0.01%)	4.21% (± 0.09%)
OT5	0.04% (± 0.06%)	29460 (± 1258)	0.04% (± 0.01%)	0.03% (± 0.00%)	2.64% (± 0.07%)	0.06% (± 0.01%)	26210 (± 1750)	0.05% (± 0.01%)	0.04% (± 0.01%)	2.75% (± 0.08%)
OT6	0.14% (± 0.12%)	30328 (± 3669)	0.11% (± 0.00%)	0.09% (± 0.01%)	2.52% (± 0.03%)	0.11% (± 0.01%)	30098 (± 1156)	0.10% (± 0.01%)	0.08% (± 0.01%)	2.41% (± 0.05%)
OT7	N/A	N/A	N/A	N/A	N/A	N/A	N/A	N/A	N/A	N/A
OT8	0.06% (± 0.09%)	26860 (± 964)	0.07% (± 0.01%)	0.04% (± 0.01%)	3.09% (± 0.11%)	0.09% (± 0.01%)	20763 (± 2487)	0.07% (± 0.01%)	0.05% (± 0.01%)	3.04% (± 0.08%)
OT9	0.07% (± 0.07%)	29898 (± 1006)	0.06% (± 0.00%)	0.05% (± 0.01%)	2.88% (± 0.12%)	0.09% (± 0.00%)	19293 (± 2664)	0.07% (± 0.01%)	0.06% (± 0.00%)	3.03% (± 0.04%)
OT10	0.13% (± 0.11%)	26198 (± 4983)	0.09% (± 0.02%)	0.08% (± 0.02%)	3.46% (± 0.14%)	0.14% (± 0.01%)	23419 (± 2369)	0.12% (± 0.01%)	0.11% (± 0.01%)	3.34% (± 0.14%)

Table S4.

Muscle weight, optimal length and cross-sectional area.

	TA muscle weight (mg)			Lo (mm)			CSA (mm^2)		
WT	54.95	±	1.51	14.37	±	0.13	6.00	±	0.14
Mdx (sham)	73.24	±	2.09*	13.95	±	0.08	8.28	±	0.21*
Mdx (treated)	54.42	±	1.56	13.61	±	0.07	6.32	±	0.20

TA, tibialis anterior
Lo, optimal muscle length
CSA, cross-sectional area
*significantly different from that of treated muscle

References and Notes

1. R. J. Fairclough, M. J. Wood, K. E. Davies, Therapy for Duchenne muscular dystrophy: Renewed optimism from genetic approaches. *Nat. Rev. Genet.* **14**, 373–378 (2013). Medline doi:10.1038/nrg3460

2. E. P. Hoffman, R. H. Brown Jr., L. M. Kunkel, Dystrophin: The protein product of the Duchenne muscular dystrophy locus. *Cell* **51**, 919–928 (1987). doi:10.1016/0092-8674(87)90579-4 Medline

3. S. B. England, L. V. Nicholson, M. A. Johnson, S. M. Forrest, D. R. Love, E. E. Zubrzycka-Gaarn, D. E. Bulman, J. B. Harris, K. E. Davies, Very mild muscular dystrophy associated with the deletion of 46% of dystrophin. *Nature* **343**, 180–182 (1990). Medline doi:10.1038/343180a0

4. B. Wang, J. Li, X. Xiao, Adeno-associated virus vector carrying human minidystrophin genes effectively ameliorates muscular dystrophy in mdx mouse model. *Proc. Natl. Acad. Sci. U.S.A.* **97**, 13714–13719 (2000). Medline doi:10.1073/pnas.240335297

5. S. Q. Harper, M. A. Hauser, C. DelloRusso, D. Duan, R. W. Crawford, S. F. Phelps, H. A. Harper, A. S. Robinson, J. F. Engelhardt, S. V. Brooks, J. S. Chamberlain, Modular flexibility of dystrophin: Implications for gene therapy of Duchenne muscular dystrophy. *Nat. Med.* **8**, 253–261 (2002). Medline doi:10.1038/nm0302-253

6. J. H. Shin, X. Pan, C. H. Hakim, H. T. Yang, Y. Yue, K. Zhang, R. L. Terjung, D. Duan, Microdystrophin ameliorates muscular dystrophy in the canine model of duchenne muscular dystrophy. *Mol. Ther.* **21**, 750–757 (2013). Medline doi:10.1038/mt.2012.283

7. J. R. Mendell, K. Campbell, L. Rodino-Klapac, Z. Sahenk, C. Shilling, S. Lewis, D. Bowles, S. Gray, C. Li, G. Galloway, V. Malik, B. Coley, K. R. Clark, J. Li, X. Xiao, J. Samulski, S. W. McPhee, R. J. Samulski, C. M. Walker, Dystrophin immunity in Duchenne's muscular dystrophy. *N. Engl. J. Med.* **363**, 1429–1437 (2010). Medline doi:10.1056/NEJMoa1000228

8. S. Cirak, V. Arechavala-Gomeza, M. Guglieri, L. Feng, S. Torelli, K. Anthony, S. Abbs, M. E. Garralda, J. Bourke, D. J. Wells, G. Dickson, M. J. Wood, S. D. Wilton, V. Straub, R. Kole, S. B. Shrewsbury, C. Sewry, J. E. Morgan, K. Bushby, F. Muntoni, Exon skipping and dystrophin restoration in patients with Duchenne muscular dystrophy after systemic phosphorodiamidate morpholino oligomer treatment: An open-label, phase 2, dose-escalation study. *Lancet* **378**, 595–605 (2011). Medline doi:10.1016/S0140-6736(11)60756-3

9. N. M. Goemans, M. Tulinius, J. T. van den Akker, B. E. Burm, P. F. Ekhart, N. Heuvelmans, T. Holling, A. A. Janson, G. J. Platenburg, J. A. Sipkens, J. M. Sitsen, A. Aartsma-Rus, G. J. van Ommen, G. Buyse, N. Darin, J. J. Verschuuren, G. V. Campion, S. J. de Kimpe, J. C. van Deutekom, Systemic administration of PRO051 in Duchenne's muscular dystrophy. *N. Engl. J. Med.* **364**, 1513–1522 (2011). Medline doi:10.1056/NEJMoa1011367

10. A. Aartsma-Rus, I. Fokkema, J. Verschuuren, I. Ginjaar, J. van Deutekom, G. J. van Ommen, J. T. den Dunnen, Theoretic applicability of antisense-mediated exon skipping for Duchenne muscular dystrophy mutations. *Hum. Mutat.* **30**, 293–299 (2009). Medline doi:10.1002/humu.20918

11. D. B. Cox, R. J. Platt, F. Zhang, Therapeutic genome editing: Prospects and challenges. *Nat. Med.* **21**, 121–131 (2015). Medline doi:10.1038/nm.3793

12. M. Jinek, K. Chylinski, I. Fonfara, M. Hauer, J. A. Doudna, E. Charpentier, A programmable dual-RNA-guided DNA endonuclease in adaptive bacterial immunity. *Science* **337**, 816–821 (2012). Medline doi:10.1126/science.1225829

13. P. Mali, L. Yang, K. M. Esvelt, J. Aach, M. Guell, J. E. DiCarlo, J. E. Norville, G. M. Church, RNA-guided human genome engineering via Cas9. *Science* **339**, 823–826 (2013). Medline doi:10.1126/science.1232033

14. L. Cong, F. A. Ran, D. Cox, S. Lin, R. Barretto, N. Habib, P. D. Hsu, X. Wu, W. Jiang, L. A. Marraffini, F. Zhang, Multiplex genome engineering using CRISPR/Cas systems. *Science* **339**, 819–823 (2013). Medline doi:10.1126/science.1231143

15. S. W. Cho, S. Kim, J. M. Kim, J. S. Kim, Targeted genome engineering in human cells with the Cas9 RNA-guided endonuclease. *Nat. Biotechnol.* **31**, 230–232 (2013). Medline doi:10.1038/nbt.2507

16. M. Jinek, A. East, A. Cheng, S. Lin, E. Ma, J. Doudna, RNA-programmed genome editing in human cells. *eLife* **2**, e00471 (2013). Medline doi:10.7554/eLife.00471

17. H. Yin, W. Xue, S. Chen, R. L. Bogorad, E. Benedetti, M. Grompe, V. Koteliansky, P. A. Sharp, T. Jacks, D. G. Anderson, Genome editing with Cas9 in adult mice corrects a disease mutation and phenotype. *Nat. Biotechnol.* **32**, 551–553 (2014). Medline doi:10.1038/nbt.2884

18. L. Swiech, M. Heidenreich, A. Banerjee, N. Habib, Y. Li, J. Trombetta, M. Sur, F. Zhang, In vivo interrogation of gene function in the mammalian brain using CRISPR-Cas9. *Nat. Biotechnol.* **33**, 102–106 (2015). Medline doi:10.1038/nbt.3055

19. R. J. Platt, S. Chen, Y. Zhou, M. J. Yim, L. Swiech, H. R. Kempton, J. E. Dahlman, O. Parnas, T. M. Eisenhaure, M. Jovanovic, D. B. Graham, S. Jhunjhunwala, M. Heidenreich, R. J. Xavier, R. Langer, D. G. Anderson, N. Hacohen, A. Regev, G. Feng, P. A. Sharp, F. Zhang, CRISPR-Cas9 knockin mice for genome editing and cancer modeling. *Cell* **159**, 440–455 (2014). Medline doi:10.1016/j.cell.2014.09.014

20. F. A. Ran, L. Cong, W. X. Yan, D. A. Scott, J. S. Gootenberg, A. J. Kriz, B. Zetsche, O. Shalem, X. Wu, K. S. Makarova, E. V. Koonin, P. A. Sharp, F. Zhang, In vivo genome editing using Staphylococcus aureus Cas9. *Nature* **520**, 186–191 (2015). Medline doi:10.1038/nature14299

21. D. G. Ousterout, A. M. Kabadi, P. I. Thakore, W. H. Majoros, T. E. Reddy, C. A. Gersbach, Multiplex CRISPR/Cas9-based genome editing for correction of dystrophin mutations that cause Duchenne muscular dystrophy. *Nat. Commun.* **6**, 6244 (2015). Medline doi:10.1038/ncomms7244

22. D. G. Ousterout, P. Perez-Pinera, P. I. Thakore, A. M. Kabadi, M. T. Brown, X. Qin, O. Fedrigo, V. Mouly, J. P. Tremblay, C. A. Gersbach, Reading frame correction by targeted genome editing restores dystrophin expression in cells from Duchenne muscular dystrophy patients. *Mol. Ther.* **21**, 1718–1726 (2013). Medline

23. L. Popplewell, T. Koo, X. Leclerc, A. Duclert, K. Mamchaoui, A. Gouble, V. Mouly, T. Voit, F. Pâques, F. Cédrone, O. Isman, R. J. Yáñez-Muñoz, G. Dickson, Gene correction of a duchenne muscular dystrophy mutation by meganuclease-enhanced exon knock-in. *Hum. Gene Ther.* **24**, 692–701 (2013). Medline doi:10.1089/hum.2013.081

24. D. G. Ousterout, A. M. Kabadi, P. I. Thakore, P. Perez-Pinera, M. T. Brown, W. H. Majoros, T. E. Reddy, C. A. Gersbach, Correction of dystrophin expression in cells from Duchenne muscular dystrophy patients through genomic excision of exon 51 by zinc finger nucleases. *Mol. Ther.* **23**, 523–532 (2015). Medline doi:10.1038/mt.2014.234

25. H. L. Li, N. Fujimoto, N. Sasakawa, S. Shirai, T. Ohkame, T. Sakuma, M. Tanaka, N. Amano, A. Watanabe, H. Sakurai, T. Yamamoto, S. Yamanaka, A. Hotta, Precise correction of the dystrophin gene in duchenne muscular dystrophy patient induced pluripotent stem cells by TALEN and CRISPR-Cas9. *Stem Cell Rev.* **4**, 143–154 (2015).doi:10.1016/j.stemcr.2014.10.013 Medline

26. P. Chapdelaine, C. Pichavant, J. Rousseau, F. Pâques, J. P. Tremblay, Meganucleases can restore the reading frame of a mutated dystrophin. *Gene Ther.* **17**, 846–858 (2010). Medline doi:10.1038/gt.2010.26

27. C. Long, J. R. McAnally, J. M. Shelton, A. A. Mireault, R. Bassel-Duby, E. N. Olson, Prevention of muscular dystrophy in mice by CRISPR/Cas9-mediated editing of germline DNA. *Science* **345**, 1184–1188 (2014). Medline doi:10.1126/science.1254445

28. L. Xu *et al*., CRISPR-mediated genome editing restores dystrophin expression and function in mdx mice. *Mol. Ther.* 10.1038/mt.2015.192 (2015). doi:10.1038/mt.2015.192

29. P. Sicinski, Y. Geng, A. S. Ryder-Cook, E. A. Barnard, M. G. Darlison, P. J. Barnard, The molecular basis of muscular dystrophy in the mdx mouse: A point mutation. *Science* **244**, 1578–1580 (1989). Medline doi:10.1126/science.2662404

30. C. J. Mann, K. Honeyman, A. J. Cheng, T. Ly, F. Lloyd, S. Fletcher, J. E. Morgan, T. A. Partridge, S. D. Wilton, Antisense-induced exon skipping and synthesis of dystrophin in the mdx mouse. *Proc. Natl. Acad. Sci. U.S.A.* **98**, 42–47 (2001). Medline doi:10.1073/pnas.98.1.42

31. A. Goyenvalle, G. Griffith, A. Babbs, S. El Andaloussi, K. Ezzat, A. Avril, B. Dugovic, R. Chaussenot, A. Ferry, T. Voit, H. Amthor, C. Bühr, S. Schürch, M. J. Wood, K. E. Davies, C. Vaillend, C. Leumann, L. Garcia, Functional correction in mouse models of muscular dystrophy using exon-skipping tricyclo-DNA oligomers. *Nat. Med.* **21**, 270–275 (2015). Medline

32. Z. Wang, T. Zhu, C. Qiao, L. Zhou, B. Wang, J. Zhang, C. Chen, J. Li, X. Xiao, Adeno-associated virus serotype 8 efficiently delivers genes to muscle and heart. *Nat. Biotechnol.* **23**, 321–328 (2005). Medline doi:10.1038/nbt1073

33. D. Li, Y. Yue, D. Duan, Marginal level dystrophin expression improves clinical outcome in a strain of dystrophin/utrophin double knockout mice. *PLOS ONE* **5**, e15286 (2010). Medline doi:10.1371/journal.pone.0015286

34. M. van Putten, M. Hulsker, C. Young, V. D. Nadarajah, H. Heemskerk, L. van der Weerd, P. A. 't Hoen, G. J. van Ommen, A. M. Aartsma-Rus, Low dystrophin levels increase survival and improve muscle pathology and function in dystrophin/utrophin double-knockout mice. *FASEB J.* **27**, 2484–2495 (2013). Medline doi:10.1096/fj.12-224170

35. M. Neri, S. Torelli, S. Brown, I. Ugo, P. Sabatelli, L. Merlini, P. Spitali, P. Rimessi, F. Gualandi, C. Sewry, A. Ferlini, F. Muntoni, Dystrophin levels as low as 30% are sufficient to avoid muscular dystrophy in the human. *Neuromuscul. Disord.* **17**, 913–918 (2007). Medline doi:10.1016/j.nmd.2007.07.005

36. Y. M. Kobayashi, E. P. Rader, R. W. Crawford, N. K. Iyengar, D. R. Thedens, J. A. Faulkner, S. V. Parikh, R. M. Weiss, J. S. Chamberlain, S. A. Moore, K. P. Campbell, Sarcolemma-localized nNOS is required to maintain activity after mild exercise. *Nature* **456**, 511–515 (2008). Medline

37. Y. Lai, G. D. Thomas, Y. Yue, H. T. Yang, D. Li, C. Long, L. Judge, B. Bostick, J. S. Chamberlain, R. L. Terjung, D. Duan, Dystrophins carrying spectrin-like repeats 16 and 17 anchor nNOS to the sarcolemma and enhance exercise performance in a mouse model of muscular dystrophy. *J. Clin. Invest.* **119**, 624–635 (2009). Medline doi:10.1172/JCI36612

38. S. Al-Zaidy, L. Rodino-Klapac, J. R. Mendell, Gene therapy for muscular dystrophy: Moving the field forward. *Pediatr. Neurol.* **51**, 607–618 (2014). Medline doi:10.1016/j.pediatrneurol.2014.08.002

39. D. Wang, H. Mou, S. Li, Y. Li, S. Hough, K. Tran, J. Li, H. Yin, D. G. Anderson, E. J. Sontheimer, Z. Weng, G. Gao, W. Xue, Adenovirus-Mediated Somatic Genome Editing of Pten by CRISPR/Cas9 in Mouse Liver in Spite of Cas9-Specific Immune Responses. *Hum. Gene Ther.* **26**, 432–442 (2015). Medline doi:10.1089/hum.2015.087

40. F. Mingozzi, K. A. High, Immune responses to AAV vectors: Overcoming barriers to successful gene therapy. *Blood* **122**, 23–36 (2013). Medline doi:10.1182/blood-2013-01-306647

41. M. Tabebordbar *et al*., In vivo gene editing in dystrophic mouse muscle and muscle stem cells. *Science* 10.1126/science.aad5177 (2015).

42. C. Long *et al*., Postnatal genome editing partially restores dystrophin expression in a mouse model of muscular dystrophy. *Science* 10.1126/science.aad5725 (2015).

43. Y. Lai, Y. Yue, M. Liu, A. Ghosh, J. F. Engelhardt, J. S. Chamberlain, D. Duan, Efficient in vivo gene expression by trans-splicing adeno-associated viral vectors. *Nat. Biotechnol.* **23**, 1435–1439 (2005). Medline doi:10.1038/nbt1153

44. P. Mali, J. Aach, P. B. Stranges, K. M. Esvelt, M. Moosburner, S. Kosuri, L. Yang, G. M. Church, CAS9 transcriptional activators for target specificity screening and paired nickases for cooperative genome engineering. *Nat. Biotechnol.* **31**, 833–838 (2013). Medline doi:10.1038/nbt.2675

45. D. Y. Guschin, A. J. Waite, G. E. Katibah, J. C. Miller, M. C. Holmes, E. J. Rebar, A rapid and general assay for monitoring endogenous gene modification. *Methods Mol. Biol.* **649**, 247–256 (2010). Medline doi:10.1007/978-1-60761-753-2_15

46. S. Bae, J. Park, J. S. Kim, Cas-OFFinder: A fast and versatile algorithm that searches for potential off-target sites of Cas9 RNA-guided endonucleases. *Bioinformatics* **30**, 1473–1475 (2014). Medline doi:10.1093/bioinformatics/btu048

47. D. Li, A. Bareja, L. Judge, Y. Yue, Y. Lai, R. Fairclough, K. E. Davies, J. S. Chamberlain, D. Duan, Sarcolemmal nNOS anchoring reveals a qualitative difference between dystrophin and utrophin. *J. Cell Sci.* **123**, 2008–2013 (2010). Medline doi:10.1242/jcs.064808

48. C. H. Hakim, N. B. Wasala, D. Duan, Evaluation of muscle function of the extensor digitorum longus muscle ex vivo and tibialis anterior muscle in situ in mice. *J. Vis. Exp.* (72): (2013). Medline